GEOLOGICA BELGICA (2014) 17/2: 137-147

Metal sources for the Katanga Copperbelt deposits (DRC): insights from Sr and Nd isotope ratios.

Jorik VAN WILDERODE[1], Hamdy A. EL DESOUKY[2], Marlina A. ELBURG[3], Frank VANHAECKE[4] & Philippe MUCHEZ[1]

[1] *Department of Earth and Environmental Sciences, KU Leuven, Celestijnenlaan 200E, 3001 Leuven, Belgium*
[2] *Geology Department, Menoufyia University, Shebin El-Kom, Egypt*
[3] *Discipline of Geological Sciences, SAEES, University of KwaZulu-Natal, Westville Campus Private Bag X54001, 4000 Durban, South-Africa*
[4] *Department of Analytical Chemistry, Ghent University, Krijgslaan 281-S12, 9000 Ghent, Belgium*

ABSTRACT. The ore deposits of the Central African Copperbelt formed during a multiphase mineralisation process. The basement underlying the Neoproterozoic Katanga Supergroup that hosts the ore, demonstrates the largest potential as metal source. Various ore deposits that formed during different mineralisation phases are taken as case studies, i.e. Kamoto, Luiswishi, Kambove West, Dikulushi and Kipushi (Democratic Republic of Congo, DRC). The Sr and Nd isotopic compositions of gangue carbonates associated with these deposits is determined and compared with those of rocks from several basement units, bordering or underlying the Copperbelt, to infer the metal sources. The mineralising fluid of diagenetic stratiform Cu-Co mineralisation interacted with felsic basement rocks underlying the region. The Co from these deposits is most likely derived from mafic rocks, but this is not observed in the isotopic signatures. Syn-orogenic, stratabound Cu-Co mineralisation resulted mainly from remobilisation of diagenetic sulphides. A limited, renewed contribution of metals from felsic basement rocks might be indicated by the isotope ratios in the western part of the Copperbelt, where the metamorphic grade is the lowest. The mineralising fluid of syn- and post-orogenic, vein-type mineralisations interacted with local mafic rocks, and with felsic basement or siliciclastic host rocks.

KEYWORDS: Sediment-hosted deposits, Vein-type deposits, Central Africa, Copper, Cobalt, Zinc

1. Introduction

The Central African Copperbelt represents a world class metallogenic province at the border between the Democratic Republic of Congo (DRC) and Zambia (Fig. 1). The orebodies are hosted by rocks of the Neoproterozoic Katanga Supergroup, which were deformed during the Lufilian orogeny (~590-530 Ma). Numerous metallogenic studies have investigated the formation of the Copperbelt ore deposits, resulting in syn-sedimentary (e.g. Garlick, 1989), early to late diagenetic (e.g. Bartholomé et al., 1972) and syn-orogenic (e.g. McGowan et al., 2003) models. An historical overview of these models has been presented by Sweeney et al. (1991) and Cailteux et al. (2005). Recently, consensus has been growing towards a multiphase mineralisation process (Selley et al., 2005; Dewaele et al., 2006; El Desouky et al., 2010; Haest & Muchez, 2011). Ore formation started with an early to intermediate diagenetic stratiform Cu-Co phase, followed by metamorphic and syn-orogenic stratabound Cu-Co mineralisation (El Desouky et al., 2010). Late to post-orogenic ore formation resulted in vein-type Cu-Zn deposits (Haest et al., 2007; Heijlen et al., 2008). Supergene remobilisation constitutes a last mineralisation phase (Decrée et al., 2010; De Putter et al., 2010). Selley et al. (2005), Kampunzu et al. (2009) and Haest & Muchez (2011) summarize the current knowledge for some of the most important ore deposits. This study addresses the possible interaction of mineralising fluids with basement units and rocks of the Katanga Supergroup to infer the most likely metal source. This is done by comparing the Sr and Nd isotopic composition of various host and basement rocks with those of gangue carbonates associated with the ore deposits (e.g. Walshaw et al., 2006).

2. Geological setting

2.1 General

The Neoproterozoic Katanga Supergroup is subdivided into the Roan, Nguba and Kundelungu Groups, and was deposited after emplacement, exhumation and erosion of the Nchanga granite

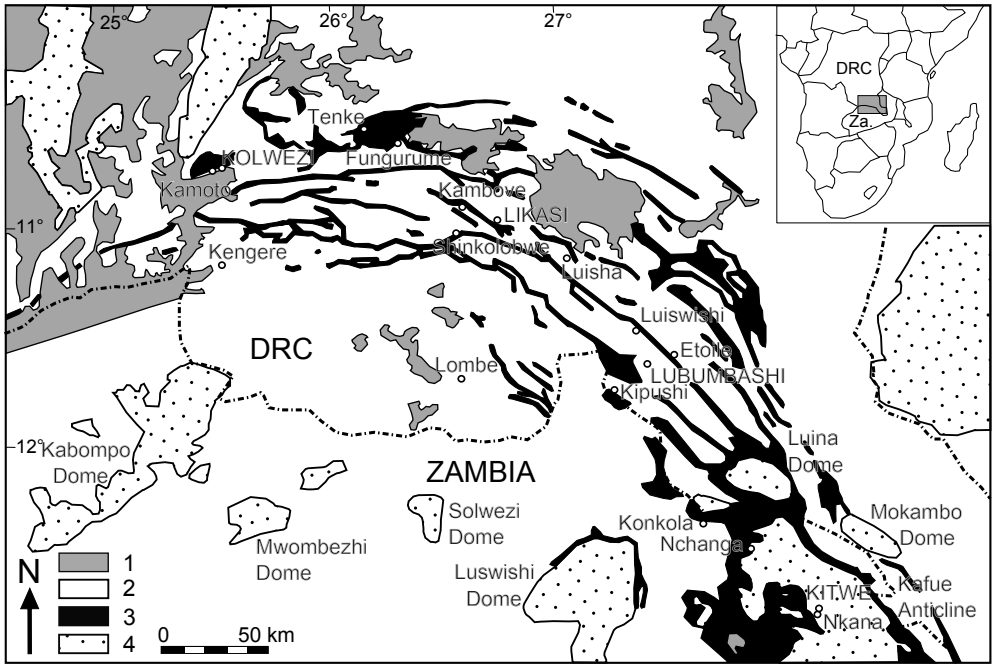

Figure 1. Geological map of the Central African Copperbelt showing the location of important ore deposits. 1: Post-Katangan rocks; 2: Mwashya, Nguba and Kundelungu rocks; 3: Faults, breccias and Roan rocks; 4: Pre-Katanga basement (after François, 1974).

Group	Subgroup	Formation	Lithology
Kundelungu (formerly Upper Kundelungu) - Ku	Biano - Ku 3		arkoses, conglomerates, argillaceous sandstones
	Ngule - Ku 2	Sampwe	dolomitic pelites, argillaceous to sandy siltstones
		Kiubo	dolomitic sandstones, siltstones and pelites
		Mongwe	dolomitic pelites, siltstones and sandstones
	Gombela - Ku 1	Lubudi	pink oolitic limestone and sandy carbonate beds
		Kanianga	carbonate siltstones and shales
		Lusele	pink to grey micritic dolomite
		Kyandamu	Petit Coglomérat (glacial diamictite)
Nguba (formerly Lower Kundelungu) - Ng	Bunkeya - Ng 2	Monwezi	dolomitic sandstones, siltstones and pelites
		Katete	dolomitic sandstones, siltstones and shales in northern areas; alternating shale and dolomite beds ("Série Récurrente") in southern areas
	Muombe (formerly "Likasi") - Ng 1	Kipushi Kakontwe Kaponda	dolomite with dolomitic shale beds in southern areas carbonates carbonate, shales and siltstones; dolomie Tigrée at the base
		Mwale	Grand Conglomérat (glacial diamictite)
Roan - R	Mwashya (old "Upper Mwashya") - R 4	Kanzadi	sandstones or alternating siltstones and shales
		Kafubu	carbonaceous shales
		Kamoya	dolomitic shales, siltstones, sandstones, including conglomeratic beds and cherts in variable positions
	Dipeta - R 3	Kansuki - R 3.4	dolomites including volcaniclastic beds (formerly "Lower Mwashya")
		Mofya - R 3.3	dolomites, arenitic dolomites, dolomitic siltstones
		R 3.2	argillaceous dolomitic siltstones with interbedded sandstone or white dolomite; intrusive gabbros
		R.G.S. - R 3.1	argillaceous dolomitic siltstones ("Roches Gréso-Schisteuses")
	Mines - R 2	Kambove - R 2.3	stromatolitic massive, laminated, shaly or talcose dolomites; locally sandstone at the base; interbedded siltstones in the upper part
		Dolomitic Shales - R 2.2	R 2.2.2 & 2.2.3: dolomitic shales containing carbonaceous horizons; occasional dolomite or arkoze R 2.2.1: arenitic dolomite at the top and dolomitic shale at the base (S.D.B.); pseudomorphs after evaporite nodules and concretions
		Kamoto - R 2.1	stromatolitic dolomite (R.S.C.), silicified/arenitic dolomites (R.S.F./D.Strat.), grey argillaceous dolomitic siltstone at the base (grey R.A.T.); pseudomorphs after evaporites at the contact with R.A.T.
	R.A.T. (Roches Argilo-Talqueuses) - R 1	R 1.3	Pink-lilac, hematitic, chloritic-dolomitic massive siltstones
		R 1.2	Pink to purple-grey, hematitic, chloritic siltstones; sandstones in the lower part; stromatolitic dolomite at top
		R 1.1	purple-red, hematitic, slightly dolomitic bedded siltstones
			Base of R.A.T. unknown in DRC

Table 1. Lithostratigraphy of the Katanga Supergroup in the DRC. S.D.B.: Shales Dolomitiques de Base; R.S.C.: Roches Siliceuse Cellulaire; R.S.F.: Roche Siliceuse Feuilletée; D. Strat.: Dolomie Stratifié (after François, 1974; Cailteux et al., 1994, 2005; Batumike et al., 2007; Kampunzu et al., 2009).

(883 ± 10 Ma; Armstrong et al., 2005). Two regional conglomerate occurrences, the Mwale and Kyandamu Formations, mark the base of the Nguba and Kundelungu Groups, respectively (Table 1). They have been correlated with the Sturtian and Marinoan glacial events (Batumike et al., 2006, 2007). Volcaniclastic rocks of the Kansuki Formation (previously known as Lower Mwashya; Cailteux et al., 2007) occur in the upper part of the underlying Roan Group. The classical stratigraphy adopted here was challenged by Wendorf (2000, 2005), however, this discussion falls outside the scope of the current study.

The Lufilian orogeny gave rise to the "Lufilian Arc" and a northern foreland known as the Kundelungu Plateau. The former is a convex belt with a total width of ~150 km and stretches for ~450 km from NW to SE. Within the arc, ore deposits are found in the external fold-and-thrust belt (DRC and Zambia), and in the adjacent Domes region (Zambia). Despite many studies (e.g. Porada, 1989; Cosi et al., 1992; Kampunzu & Cailteux, 1999; Jackson et al., 2003), the timing and mode of deformation remains an important discussion. Nevertheless, early and peak metamorphism can be set at ~590 Ma (Rainaud et al., 2005) and ~530 Ma (John et al., 2004; Rainaud et al., 2005), respectively. The main deformation period likely started around 560 Ma, which is the age of syn-orogenic granites (Hanson et al., 1993; Porada & Berhorst, 2000). However, Lufilian deformation probably did not affect the Kundelungu plateau before 525 Ma (Haest et al., 2009b).

The Lufilian orogen is surrounded by the Kibara Belt in the NW, the Bangweulu Block in the NE and the Irumide Belt in the East (Fig. 2). The Kibara orogen was active between ~1.4-1.38 Ga (accretionary stage) and ~1.0-0.95 Ga (continental collision; Kokonyangi et al., 2006). The oldest of four meta-sedimentary groups composing the Kibara Supergroup was affected by arc-related calc-alkaline and peraluminous magmatism at 1.38 Ga (Kokonyangi et al., 2006; Tack et al., 2010). Late to post-orogenic granites and pegmatites, formed after 1.0 Ga, host Sn and W deposits (Kokonyangi et al., 2006; Tack et al., 2010; Dewaele et al., 2011). The apparent northern continuation of the Kibara Belt was previously known as the North-Eastern Kibara Belt, but was redefined by Tack et al. (2010) as the Karagwe-Ankole Belt. The Palaeoproterozoic Bangweulu Block contains a granitoid basement and a cover of mainly fluvial, aeolian and lacustrine sediments (Andersen & Unrug, 1984). De Waele et al. (2006) recognised four main igneous phases in the Irumide Belt and interpreted this belt as the repeatedly destabilised southern boundary of the Bangweulu Block. The destabilisation occurred at 2.0, 1.85, 1.6 and 1.0 Ga. The meta-sedimentary cover consists of alternating quartzites and pelites (De Waele & Mapani, 2002; De Waele & Fitzsimons, 2007). Within the Lufilian Arc, basement is cropping out in the Domes Region and was dated at 1.88 Ga (Ngoyi et al., 1991). Taking into account regional age data, Ngoyi et al. (1991), Ngoyi & Dejonghe (1995) and De Waele et al. (2006) consider the doming basement to be part of a Bangweulu Metacraton. This Bangweulu Metacraton acted as a basement to the Lufilian Belt and underlies the largest part of the Copperbelt (De Waele et al., 2006).

2.2 The Kamoto, Luiswishi and Kambove deposits

The Kamoto Cu-Co deposit is part of the Kolwezi megabreccia klippe, located in the north-western part of the Copperbelt (Fig. 1). It presumably represents a remnant of a thrust sheet and contains faulted blocks forming isoclinal folds (François, 1974). The Kambove West Cu-Co mineralisation occurs in the central part of the Copperbelt (Fig. 1) within a north-verging syncline (Cailteux, 1983). The Luiswishi Cu-Co deposit is situated in the eastern part of the Congolese Copperbelt (Fig. 1) and occurs in a fractured, north-verging isoclinal synform (Cailteux et al., 2003). The main mineralisation at these deposits is hosted by the lower parts of the Kamoto and Dolomitic Shales Formations (Table 1; Cailteux et al., 2005). The Lower and Upper Orebodies are separated by the

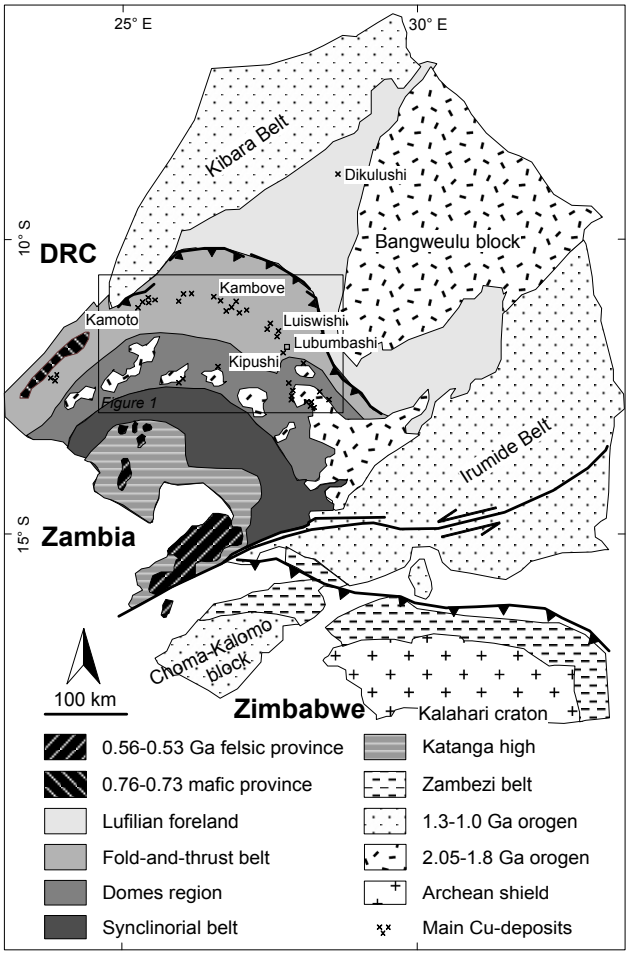

Figure 2. The Lufilian orogen and surrounding tectonic units (after Selley et al., 2005; De Waele et al., 2006).

generally barren R.S.C. Member (Roches Siliceuses Cellulaires), a massive silicified stromatolitic dolomite.

The first stratiform hydrothermal Cu-Co mineralisation phase at Kamoto, Luiswishi and Kambove West produced fine- to medium-grained sulphides that occur disseminated, within small nodules and in thin, discontinuous layers (Muchez et al., 2008; Van Langendonck et al., 2013). Mineralisation took place during diagenesis of the host rocks from a moderate saline fluid (11.3-20.9 wt.% NaCl equiv.) at a temperature between 115 and 220°C (El Desouky et al., 2009). The R.S.C. member might have acted as a conduit for this mineralising fluid (Fay & Barton, 2012; Muchez & Corbella, 2012). Sulphides display $\delta^{34}S$ values between -10.3 and +3.1 ‰ V-CDT, corresponding to a fractionation of 14.4 to 27.8 ‰ from Neoproterozoic seawater sulphate (Muchez et al., 2008). Such large fractionation suggests bacterial mediated sulphate reduction (BSR).

The second Cu-Co mineralisation phase at Kamoto, Luiswishi and Kambove West took place during the Lufilian Orogeny. It formed coarse-grained sulphide minerals in veins, breccia cements and nodules with varying shapes (El Desouky et al., 2010; Van Langendonck et al., 2013). The mineralising fluid was highly saline (35-45.5 wt.% NaCl equiv.) and hot (270-385°C; El Desouky et al., 2009). Most $\delta^{34}S$ values range from -13.1 to +5.2 ‰ V-CDT, comparable to the $\delta^{34}S$ signature of the first mineralisation phase. A few sulphides display higher $\delta^{34}S$ values between +18.6 and +21.0 ‰ V-CDT (El Desouky et al., 2010). As BSR is not possible at the high temperature of the second mineralisation phase, the former range indicates remobilisation of sulphur from first phase sulphides. The latter range resembles the marine seawater $\delta^{34}S$ signature between 840 Ma and the Sturtian Glaciation around ~700 Ma (+17.5 to +19.0 ‰ V-CDT; Veizer et al., 1980; Gorjan et al., 2000; Hurtgen et al., 2002, 2005) and points to thermochemical sulphate reduction (TSR).

2.3 The Dikulushi and Kipushi deposits

The Dikulushi Cu-Ag mineralisation is a vein-type deposit found about 200 km north of the Copperbelt in the foreland of the Lufilian orogen (Fig. 2). The host rocks belong to the Lubudi and Mongwe Formations (Table 1; Cailteux et al., 2005). A syn-orogenic, moderately saline (20-25 wt.% $CaCl_2$ equiv.) and warm (90-140°C) fluid precipitated Cu-Pb-Zn-Fe ore in a zone of crosscutting east and north-east oriented faults (Haest et al., 2009b). A post-orogenic, saline (≥ 19 wt.% NaCl equiv.) and low temperature (~65°C) fluid subsequently remobilised ore metals along north-eastern oriented faults and caused Cu-Ag mineralisation after mixing with a low saline (≤ 3 wt.% NaCl equiv.) fluid. This event may have occurred only ca. 100 Ma ago (Haest et al., 2009b). $\delta^{34}S$ values for sulphides of the first and second mineralisation phase are similar, i.e. +11.3 to +14.1 ‰ and +10.0 to +13.5 ‰ V-CDT, respectively (Haest et al., 2009b). This indicates TSR for the former and remobilisation of first phase sulphides at a low temperature during the second mineralisation phase.

The Kipushi vein-type Cu-Zn deposit is positioned in the south-eastern part of the Katanga Copperbelt (Fig. 1) within the northern flank of a NW-SE trending anticline. The anticlinal core consists of a megabreccia of Roan Group rocks known as the Axial Breccia (De Magnée & François, 1988). The pipe-like ore-body crosscuts rocks of the Kakontwe, Kipushi and Katete Formations (Table 1; Batumike et al., 2007), and was dated at 450.5 ± 3.4 Ma (Schneider et al., 2007). The main mineralisation phase formed from a highly saline (30-43 wt.% NaCl equiv.) and hot (287-331°C) fluid (Chabu, 1995; Heijlen et al., 2008). A fluid of lower salinity (~23-31 wt% NaCl equiv.) and temperature (<170°C) caused a minor secondary mineralisation phase (Heijlen et al., 2008). $\delta^{34}S$ signatures of the ore-body demonstrate that the major part of the sulphides was derived from seawater sulphate through TSR (up to +19.2 ‰ V-CDT), while a small part was inherited from BSR (down to -2.6 ‰ V-CDT; Dechow & Jensen, 1965).

3. Possible metal sources

A magmatic-hydrothermal metal source for the Copperbelt deposits was favoured by early workers (e.g. Bateman, 1930), but refuted by the presence of unconformable sediment-granite contacts (Garlick & Brummer, 1951) and granite dating (e.g. Armstrong et al., 2005). Oxidised siliciclastic sediments or red beds of the R.A.T. Subgroup (Roan Group) formed in an early rift basin and underlie the mineralised strata (Table 1; Kampunzu et al., 2000). This configuration mimics other important sediment-hosted stratiform Cu provinces, like the Permian basin of Central Europe (e.g. Hitzman et al., 2005). Red beds contain feldspars, metals absorbed on amorphous iron oxides and often detrital mafic minerals, providing an excellent source for ore metals (e.g. Brown, 1984; Schuh et al., 2012). However, Hitzman (2000) assessed the volume of red beds underlying or lateral to the Zambian Copperbelt, and found a deficiency in red bed volume to account for the known mineralisations. Similarly, Cailteux et al. (2005) calculated that at least 100 times the volume of footwall sedimentary rocks in the Lufilian Arc is required to provide sufficient amounts of copper. Several authors mentioned the possibility of a metal contribution from a larger part of the local stratigraphy (e.g. De Magnée & Francois 1988; Lefebvre, 1989), although Selley et al. (2005) considered it rather unlikely due to an insufficient sedimentary rock volume. Hitzman (2000) argued in favour of significant tectonic displacement of the ore-bearing strata from a south-western source basin. However, structurally conformable contacts both within the Katanga Supergroup and between basement and basinal strata do not concur with such displacement (Koziy et al., 2009).

Unlike other possibilities, the basement provides great potential as a metal source (e.g. Sweeney et al., 1991; Sweeney & Binda, 1994; Roberts et al., 2009). Metal sulphide occurrences are reported within the basement at Samba, Lumwana, Mkushi and elsewhere (e.g. Schneiderhöhn, 1937; Pienaar, 1961; Omenetto, 1973; Whyte and Green, 1971; Wakefield, 1978; Sweeney et al., 1991; Bernau et al., 2013). For the cases where they underlie sediment-hosted orebodies, Whyte and Green (1971) suggested that these occurrences might be the result of downward migration of metals into the basement. The basement-hosted mineralisations are mostly found close to the basal unconformity of the Katanga Supergroup and contain similar gangue assemblages as found in sediment-hosted deposits. Therefore, Selley et al. (2005) considered them a correlative rather than a possible source to the sediment-hosted deposits. Even so, a high Cu and Co content is found in basement granitoids even when no sulphides are present. Sweeney et al. (1991) listed recorded metal concentrations of several hundreds of ppm of Cu and Co in basement rocks, reviewing data from amongst others Pienaar (1961), Mendelsohn (1961) and Garlick (1973). These rocks might be source rocks, since numerical modelling for the Zambian Copperbelt shows that buoyancy-driven fluid flow across the basin-basement contact is very well possible, even with a low-permeable basement and without the presence of major vertical fault systems (Koziy et al., 2009).

The potential of the basement is supported by the co-variation of the Pb isotopic composition of Cu and Co-sulphides from various mineralisations and basement schists and granites underlying those various deposits (Carr et al., 1987). The same authors and Richards et al. (1988) used Pb isotopic compositions to demonstrate that mantle-derived basement rocks were no metal source to the stratiform deposits. Kamona et al. (1999) argues in favour of a mantle component for the Kipushi vein-type Cu-Zn deposit. However, this is refuted by Schneider et al. (2007), who confirm a crustal reservoir as metal source for Kipushi based upon Pb isotopic signatures and initial $^{87}Sr/^{86}Sr$ and $^{187}Os/^{188}Os$ ratios. Implicit in these studies is the assumption that both Pb and other ore metals originated from the same source. Furthermore, taking into account the high mobility of Pb and U, the Pb isotopic signatures should be interpreted with caution (e.g. Decrée et al., 2011).

Despite the apparent granitic association (Carr et al., 1987) and the paucity of mafic rocks in the area, the high Co grades in the stratiform ores are thought to originate from a mafic source rock (e.g. Annels et al., 1983; Annels & Simmonds, 1984; Unrug, 1988; Annels, 1989). Starting from a basement with 20 percent mafic and 80 percent felsic rocks, Koziy et al. (2009) model that only 40 percent of the Cu in the basement rocks affected by a high water-rock ratio needs to be leached to account for the Zambian ore deposits. Hence, the volume of source rocks

is much less an issue in the case of the basement than it is for continental red beds. Also Muchez & Corbella (2012) address the importance of mafic source rocks. They successfully simulate the general paragenetic evolution of stratiform Cu-Co deposits in the Katanga Copperbelt after the reaction of an evaporated sea water fluid with both mafic and granitic rocks. Unrug (1988) considers volcaniclastic rocks within the Nguba Group (formerly Lower Kundelungu) and gabbro-dolerite sills throughout the Lufilian orogen abundant enough for acting as metal source. However, the problem of whether their volume proves sufficient is compounded by the fact that these rocks were not yet formed during early diagenetic mineralisation (Sweeney & Binda, 1989; Cailteux et al., 2005). Annels (1974), Annels et al. (1983), and Annels and Simmonds (1984) also note this presence of amphibolite bodies close to stratiform Cu deposits, but at higher stratigraphic levels within the Roan Group. They suggested a common deep seated and rift-related mafic source for the amphibolites and the cobalt in the stratiform orebodies. However, the Pb isotopic signatures of the gabroic bodies do not correspond with Pb signatures from stratiform sulphides (Carr et al., 1987).

Location	Timing/ ID	Mineralisation	Gangue type/ stratigraphy	Rb (µg/g)	2s	Sr (µg/g)	2s	$^{87}Sr/^{86}Sr$	2s	$^{87}Rb/^{86}Sr$	$^{87}Sr/^{86}Sr$ 816 Ma	2s	$^{87}Sr/^{86}Sr$ 590 Ma	2s	$^{87}Sr/^{86}Sr$ 525 Ma	2s	$^{87}Sr/^{86}Sr$ 451 Ma	2s	$^{87}Sr/^{86}Sr$ 100 Ma	2s
	Post-orogenic																			
Dikulushi	DI03WH11	Cu-Ag	Cal 3	0.028	0.002	535	8	0.71448	0.00001	0.0002	na	na	na	na	na	na	na	na	0.71448	0.00001
Dikulushi	DI03WH21	Cu-Ag	Cal 3	0.114	0.002	375	6	0.71610	0.00001	0.0009	na	na	na	na	na	na	na	na	0.71610	0.00001
Dikulushi	DI04MH32	Cu-Ag	Cal 3	0.268	0.003	124	2	0.71359	0.00001	0.0063	na	na	na	na	na	na	na	na	0.71358	0.00001
Dikulushi	DI04MH42	Cu-Ag	Cal 3	0.126	0.002	141	2	0.71487	0.00001	0.0026	na	na	na	na	na	na	na	na	0.71487	0.00001
Kipushi	KI04HC01	Cu-Zn	Dol vein	0.114	0.001	69.4	0.7	0.71303	0.00001	0.0047	na	na	na	na	na	na	0.71300	0.00001	na	na
Kipushi	KI04HC02	Cu-Zn	Dol vein	0.230	0.003	135	1	0.71209	0.00001	0.0049	na	na	na	na	na	na	0.71206	0.00001	na	na
Kipushi	KI04HC07	Cu-Zn	Dol vein	0.384	0.004	78.3	0.7	0.71303	0.00001	0.0142	na	na	na	na	na	na	0.71294	0.00001	na	na
Kipushi	KI04HC10	Cu-Zn	Dol vein	0.068	0.001	94	1	0.71063	0.00002	0.0021	na	na	na	na	na	na	0.71061	0.00002	na	na
Kipushi	KI04HC15	Cu-Zn	Dol vein	0.861	0.009	232	2	0.71123	0.00002	0.0108	na	na	na	na	na	na	0.71117	0.00002	na	na
Kipushi	KI04HC16	Cu-Zn	Dol vein	0.677	0.007	264	3	0.71110	0.00001	0.0074	na	na	na	na	na	na	0.71105	0.00001	na	na
Kipushi	KI04HC20	Cu-Zn	Dol vein	0.539	0.006	151	2	0.71339	0.00001	0.0103	na	na	na	na	na	na	0.71332	0.00001	na	na
Kipushi	KI04HC28	Cu-Zn	Dol vein	0.741	0.007	491	5	0.71272	0.00001	0.0044	na	na	na	na	na	na	0.71269	0.00001	na	na
Kipushi	KI04HC59	Cu-Zn	Dol vein	0.566	0.006	594	6	0.71118	0.00001	0.0028	na	na	na	na	na	na	0.71116	0.00001	na	na
	Syn-orogenic																			
Dikulushi	DI04MH11	Cu-Pb-Zn-Fe	Cal 1	0.034	0.001	539	8	0.71400	0.00001	0.0002	na	na	na	na	0.71400	0.00001	na	na	0.71400	0.00001
Dikulushi	DI04MH17	Cu-Pb-Zn-Fe	Cal 1	0.054	0.002	266	4	0.71270	0.00001	0.0006	na	na	na	na	0.71270	0.00001	na	na	0.71270	0.00001
Dikulushi	DI04MH40	Cu-Pb-Zn-Fe	Dol 3	0.188	0.004	77	1	0.71349	0.00001	0.0071	na	na	na	na	0.71344	0.00001	na	na	0.71348	0.00001
Dikulushi	DI06MH09	Cu-Pb-Zn-Fe	Cal 1	0.183	0.002	450	7	0.71463	0.00001	0.0012	na	na	na	na	0.71462	0.00001	na	na	0.71463	0.00001
Dikulushi	DI06MH34	Cu-Pb-Zn-Fe	Dol 3	0.176	0.002	125	2	0.71377	0.00003	0.0041	na	na	na	na	0.71374	0.00003	na	na	0.71376	0.00003
Dikulushi	DI06MH89	Cu-Pb-Zn-Fe	Dol 3	0.276	0.004	403	6	0.71534	0.00002	0.0020	na	na	na	na	0.71533	0.00002	na	na	0.71534	0.00002
Dikulushi	DI06MH143	Cu-Pb-Zn-Fe	Cal 1	0.080	0.002	187	3	0.71343	0.00002	0.0012	na	na	na	na	0.71342	0.00002	na	na	0.71343	0.00002
Kambove	KW11SL01	Cu-Co	Dol III	1.14	0.02	108	2	0.70926	0.00010	0.0305	na	na	0.70901	0.00010	0.70903	0.00010	na	na	na	na
Kambove	KW11SL02	Cu-Co	Dol III	0.411	0.008	55	1	0.70977	0.00009	0.0215	na	na	0.70959	0.00009	0.70961	0.00009	na	na	na	na
Kambove	KW11SL03	Cu-Co	Dol III	0.66	0.01	72	2	0.70939	0.00010	0.0263	na	na	0.70917	0.00010	0.70920	0.00010	na	na	na	na
Kambove	KW11SL05	Cu-Co	Dol III	0.66	0.01	71	1	0.71001	0.00011	0.0271	na	na	0.70979	0.00011	0.70981	0.00011	na	na	na	na
Kambove	KW11SL09	Cu-Co	Dol III	0.60	0.01	73	2	0.70912	0.00009	0.0238	na	na	0.70892	0.00009	0.70894	0.00009	na	na	na	na
Kambove	KW11SL25	Cu-Co	Dol III	0.419	0.008	53	1	0.70952	0.00007	0.0228	na	na	0.70933	0.00008	0.70935	0.00008	na	na	na	na
Kambove	KW11SL43	Cu-Co	Dol III	0.82	0.02	78	2	0.70913	0.00009	0.0305	na	na	0.70887	0.00009	0.70890	0.00009	na	na	na	na
Luiswishi	LS06HA009[1]	Cu-Co	Nod II	unk	unk	64.6	0.7	0.71119	0.00001	unk	na	na	0.71119	0.00001	0.71119	0.00001	na	na	na	na
Luiswishi	LS06HA016[1]	Cu-Co	Dol vein	unk	unk	30.2	0.3	0.71013	0.00002	unk	na	na	0.71013	0.00002	0.71013	0.00002	na	na	na	na
Luiswishi	LS06HA023	Cu-Co	Dol vein	0.58	0.01	15.0	0.2	0.71137	0.00002	0.1110	na	na	0.71044	0.00007	0.71054	0.00007	na	na	na	na
Luiswishi	LS06HA037	Cu-Co	Breccia	1.49	0.03	20.1	0.2	0.71215	0.00002	0.2150	na	na	0.71034	0.00014	0.71054	0.00013	na	na	na	na
Luiswishi	LS06HA040[1]	Cu-Co	Nod II	unk	unk	21.1	0.2	0.71046	0.00004	unk	na	na	0.71046	0.00004	0.71046	0.00004	na	na	na	na
Luiswishi	LS06HA043	Cu-Co	Nod II	0.398	0.008	10.0	0.1	0.71032	0.00001	0.1150	na	na	0.70935	0.00008	0.70946	0.00007	na	na	na	na
Luiswishi	LS06HA060[1]	Cu-Co	Breccia	unk	unk	47.1	0.5	0.71004	0.00002	unk	na	na	0.71004	0.00002	0.71004	0.00002	na	na	na	na
Luiswishi	LS06HA064[1]	Cu-Co	Breccia	unk	unk	61.7	0.7	0.71001	0.00002	unk	na	na	0.71001	0.00002	0.71001	0.00002	na	na	na	na
Luiswishi	LS06HA070	Cu-Co	Dol vein	0.48	0.01	19.9	0.2	0.71094	0.00001	0.0700	na	na	0.71035	0.00005	0.71042	0.00004	na	na	na	na
Luiswishi	LS06HA108[1]	Cu-Co	Dol vein	unk	unk	24.1	0.3	0.71002	0.00001	unk	na	na	0.71002	0.00001	0.71002	0.00001	na	na	na	na
Kamoto	KA05VD052	Cu-Co	Dol vein	0.443	0.009	26.0	0.3	0.70952	0.00002	0.0490	na	na	0.70911	0.00004	0.70915	0.00004	na	na	na	na
Kamoto	KA05VD067	Cu-Co	Dol vein	0.355	0.007	33.7	0.4	0.70933	0.00001	0.0300	na	na	0.70908	0.00002	0.70911	0.00002	na	na	na	na
Kamoto	KA07HA01[1]	Cu-Co	Nod II	unk	unk	42.3	0.5	0.70919	0.00001	unk	na	na	0.70919	0.00001	0.70919	0.00001	na	na	na	na
Kamoto	KA07HA05[1]	Cu-Co	Dol vein	unk	unk	40.2	0.4	0.70926	0.00002	unk	na	na	0.70926	0.00002	0.70926	0.00002	na	na	na	na
Kamoto	KA07HA15	Cu-Co	Breccia	0.023	0.001	5.85	0.06	0.70883	0.00002	0.0110	na	na	0.70874	0.00002	0.70875	0.00002	na	na	na	na
	Diagenetic																			
Luiswishi	LS06HA005	Cu-Co	Nod/layers I	0.52	0.01	33.1	0.4	0.71104	0.00002	0.0460	0.71050	0.00005	0.71065	0.00004	0.71070	0.00003	na	na	na	na
Luiswishi	LS06HA034[1]	Cu-Co	Nod/layers I	unk	unk	11.4	0.1	0.71090	0.00002	unk	0.71090	0.00002	0.71090	0.00002	0.71090	0.00002	na	na	na	na
Luiswishi	LS06HA067	Cu-Co	Nod/layers I	0.109	0.002	2.42	0.03	0.71046	0.00001	0.1300	0.70894	0.00012	0.70937	0.00009	0.70949	0.00008	na	na	na	na
Luiswishi	LS06HA080[1]	Cu-Co	Nod/layers I	unk	unk	22.5	0.2	0.71022	0.00003	unk	0.71022	0.00003	0.71022	0.00003	0.71022	0.00003	na	na	na	na
Luiswishi	LS06HA0107[1]	Cu-Co	Nod/layers I	unk	unk	30.2	0.3	0.70987	0.00001	unk	0.70987	0.00001	0.70987	0.00001	0.70987	0.00001	na	na	na	na
Kamoto	KA05VD011[1]	Cu-Co	Nod/layers I	unk	unk	31.2	0.2	0.71025	0.00002	unk	0.71025	0.00002	0.71025	0.00002	0.71025	0.00002	na	na	na	na
Kamoto	KA05VD012	Cu-Co	Nod/layers I	0.0240	0.0003	16.1	0.1	0.71120	0.00018	0.0043	0.71115	0.00018	0.71116	0.00018	0.71117	0.00018	na	na	na	na
Kamoto	KA05VD062[1]	Cu-Co	Nod/layers I	unk	unk	29.3	0.2	0.71024	0.00002	unk	0.71024	0.00002	0.71024	0.00002	0.71024	0.00002	na	na	na	na
Kamoto	KA05VD065[1]	Cu-Co	Nod/layers I	unk	unk	40.6	0.3	0.71223	0.00003	unk	0.71223	0.00003	0.71223	0.00003	0.71223	0.00003	na	na	na	na
Kamoto	KA05VD066[1]	Cu-Co	Nod/layers I	unk	unk	41.1	0.2	0.71012	0.00001	unk	0.71012	0.00001	0.71012	0.00001	0.71012	0.00001	na	na	na	na
Kamoto	KA07HA04	Cu-Co	Nod/layers I	0.044	0.001	7.13	0.05	0.71021	0.00002	0.0177	0.71000	0.00002	0.71006	0.00002	0.71008	0.00002	na	na	na	na
Kamoto	KA07HA18[1]	Cu-Co	Nod/layers I	unk	unk	19.8	0.1	0.71309	0.00002	unk	0.71309	0.00002	0.71309	0.00002	0.71309	0.00002	na	na	na	na
Kamoto	KA07HA20	Cu-Co	Nod/layers I	0.083	0.001	18.51	0.08	0.73408	0.00002	0.0130	0.73393	0.00002	0.73397	0.00002	0.73398	0.00002	na	na	na	na
Kamoto	KA07HA21	Cu-Co	Nod/layers I	0.718	0.007	22.3	0.1	0.73576	0.00002	0.0933	0.73467	0.00004	0.73498	0.00003	0.73506	0.00003	na	na	na	na
Kamoto	KA07HA22	Cu-Co	Nod/layers I	0.132	0.002	14.8	0.1	0.71493	0.00001	0.0260	0.71463	0.00002	0.71471	0.00001	0.71474	0.00001	na	na	na	na
Kamoto	KA07HA24	Cu-Co	Nod/layers I	0.811	0.008	41.9	0.3	0.71038	0.00003	0.0561	0.70973	0.00004	0.70991	0.00004	0.70996	0.00003	na	na	na	na
Kamoto	KA07HA28	Cu-Co	Nod/layers I	1.064	0.009	33.2	0.2	0.71332	0.00002	0.0928	0.71224	0.00004	0.71254	0.00003	0.71263	0.00003	na	na	na	na
	Host rocks																			
Kipushi	KI09JV34	na	Katete Fm	3.98	0.03	105	1	0.71235	0.00006	0.1071	na	na	na	na	na	na	0.71166	0.00007	na	na
Kipushi	KI09JV03	na	Kakontwe Fm	0.282	0.009	79	1	0.70867	0.00006	0.0101	na	na	na	na	na	na	0.70861	0.00006	na	na
Kipushi	KI09JV07	na	Kakontwe Fm	0.184	0.002	67.6	0.6	0.70958	0.00006	0.0077	na	na	na	na	na	na	0.70953	0.00006	na	na
Kipushi	KI09JV12	na	Kakontwe Fm	5.4	0.2	134	4	0.71074	0.00006	0.1131	na	na	na	na	na	na	0.71001	0.00012	na	na
Kipushi	KI09JV17	na	Kakontwe Fm	0.39	0.02	93.8	0.8	0.70801	0.00006	0.0118	na	na	na	na	na	na	0.70793	0.00006	na	na
Kipushi	KI09JV20	na	Kakontwe Fm	0.209	0.009	92	1	0.70895	0.00006	0.0064	na	na	na	na	na	na	0.70891	0.00006	na	na
Kipushi	KI09JV22	na	Kakontwe Fm	0.47	0.02	84	1	0.70846	0.00006	0.0158	na	na	na	na	na	na	0.70836	0.00006	na	na
Kipushi	KI09JV29	na	Kakontwe Fm	2.33	0.06	205	9	0.70924	0.00006	0.0321	na	na	na	na	na	na	0.70903	0.00007	na	na
Kipushi	KI09JV52	na	Kakontwe Fm	2.11	0.02	73	1	0.70921	0.00006	0.0819	na	na	na	na	na	na	0.70868	0.00007	na	na
Kipushi	KI09JV56	na	Kakontwe Fm	1.96	0.05	89	1	0.71086	0.00006	0.0623	na	na	na	na	na	na	0.71046	0.00008	na	na
Kipushi	KI09JV59	na	Kakontwe Fm	13.9	0.2	187	8	0.70969	0.00006	0.2101	na	na	na	na	na	na	0.70834	0.00020	na	na
Kipushi	KI09JV65	na	Kakontwe Fm	0.94	0.03	145	2	0.70839	0.00006	0.0183	na	na	na	na	na	na	0.70827	0.00006	na	na
Kipushi	KI09JV138	na	Kakontwe Fm	1.56	0.03	136	3	0.70956	0.00006	0.0323	na	na	na	na	na	na	0.70935	0.00007	na	na
Kipushi	KI09JV163	na	Kakontwe Fm	0.54	0.01	69.1	0.5	0.70831	0.00006	0.0219	na	na	na	na	na	na	0.70817	0.00006	na	na
Kipushi	KI09JV167	na	Kakontwe Fm	8.96	0.05	97	2	0.71032	0.00006	0.2610	na	na	na	na	na	na	0.70864	0.00012	na	na
Kipushi	KI04HC14	na	Kakontwe Fm	2.63	0.03	160	2	0.70941	0.00003	0.0475	na	na	na	na	na	na	0.70910	0.00003	na	na
Kipushi	KI04HC39	na	Kakontwe Fm	0.946	0.009	177	2	0.70880	0.00001	0.0155	na	na	na	na	na	na	0.70870	0.00001	na	na
Kipushi	KI04HC49	na	Kakontwe Fm	0.0454	0.0005	127	1	0.70811	0.00001	0.0010	na	na	na	na	na	na	0.70811	0.00001	na	na
Kakontwe	RG157650	na	Kakontwe Fm	0.82	0.02	293	6	0.70797	0.00008	0.0080	na	na	na	na	na	na	0.70792	0.00008	na	na
Kakontwe	RG157656	na	Kakontwe Fm	0.427	0.008	647	14	0.70748	0.00009	0.0019	na	na	na	na	na	na	0.70747	0.00009	na	na
Dikulushi	DI06MH83	na	Gombela Sbgr	22.7	0.3	50.1	0.8	0.72209	0.00001	1.3200	na	na	na	na	0.71221	0.00072	na	na	0.72021	0.00014
Dikulushi	DI06MH107	na	Gombela Sbgr	27.5	0.4	39.4	0.6	0.73171	0.00003	2.0300	na	na	na	na	0.71652	0.00113	na	na	0.72883	0.00022
Dikulushi	DI06MH108	na	Gombela Sbgr	10.9	0.1	53.8	0.8	0.71425	0.00002	0.5900	na	na	na	na	0.70984	0.00026	na	na	0.71341	0.00005
S-Katanga	RG157635	na	Gombela Sbgr	11.3	0.2	221	5	0.71134	0.00007	0.1478	na	na	na	na	0.71024	0.00013	na	na	0.71113	0.00007
Shituru	RG157670	na	Mwashya volc	0.504	0.009	11.6	0.2	0.71405	0.00010	0.1261	na	na	0.71299	0.00015	0.71311	0.00014	0.71324	0.00013	na	na
Shituru	RG157672	na	Mwashya volc	1.08	0.02	5.4	0.1	0.71811	0.00019	0.5784	na	na	0.71324	0.00052	0.71378	0.00047	0.71439	0.00041	na	na
S-Katanga	RG157668	na	Mwashya Sbgr	10.4	0.2	209	4	0.70916	0.00009	0.1439	na	na	0.70795	0.00015	0.70808	0.00014	na	na	na	na
Kabolela	KB08HA02	na	Dipeta Sbgr	2.17	0.05	109	1	0.70796	0.00002	0.0578	na	na	0.70747	0.00005	0.70753	0.00004	na	na	na	na
Kabolela	KB08HA03	na	Dipeta Sbgr	0.78	0.02	88	1	0.70927	0.00002	0.0254	na	na	0.70906	0.00003	0.70908	0.00003	na	na	na	na
Kabolela	KB08HA06	na	Dipeta Sbgr	8.8	0.2	255	4	0.70774	0.00002	0.1000	na	na	0.70690	0.00008	0.70699	0.00007	na	na	na	na
S-Katanga	RG157674	na	Dipeta Sbgr	0.460	0.009	1619	34	0.70620	0.00010	0.0008	na	na	0.70619	0.00010	0.70619	0.00010	na	na	na	na
S-Katanga	RG157675	na	Dipeta Sbgr	1.10	0.02	249	5	0.70886	0.00007	0.0128	na	na	0.70875	0.00007	0.70876	0.00007	na	na	na	na
Kambove	KM08HA01	na	Mines Sbgr	4.14	0.08	265	6	0.70738	0.00007	0.0452	0.70686	0.00009	0.70700	0.00008	0.70705	0.00008	na	na	na	na
Kambove	KM08HA02	na	Mines Sbgr	8.1	0.2	331	7	0.70772	0.00007	0.0706	0.70690	0.00011	0.70712	0.00009	0.70719	0.00009	na	na	na	na
Kamoto	KA05VD081	na	Dol Shales Fm	0.57	0.01	34.2	0.5	0.70904	0.00001	0.0484	0.70848	0.00005	0.70863	0.00004	0.70868	0.00003	na	na	na	na
Luiswishi	LS11PM07	na	Kamoto Fm	0.485	0.009	66	1	0.71014	0.00010	0.0212	0.70990	0.00010	0.70996	0.00010	0.70998	0.00010	na	na	na	na
Luiswishi	LS11PM37	na	Kamoto Fm	0.187	0.003	2.22	0.05	0.71034	0.00024	0.2431	0.70751	0.00037	0.70830	0.00032	0.70852	0.00030	na	na	na	na
Luiswishi	LS11PM38	na	Kamoto Fm	0.092	0.002	6.7	0.1	0.71010	0.00010	0.0397	0.70963	0.00011	0.70976	0.00011	0.70980	0.00011	na	na	na	na
Kamoto	KA12DD02	na	Kamoto Fm	0.84	0.02	20.4	0.4	0.70990	0.00010	0.1191	0.70851	0.00017	0.70890	0.00014	0.70901	0.00013	na	na	na	na

Table 2. Rb-Sr results with recalculation of the isotopic compositions at 816, 590, 525 and 451 Ma. [1]: no age correction applied because of extreme Sr/Rb ratios of these pure carbonates; Dol: dolomite; Cal: calcite; Nod: nodules; Sbgr: Subgroup; Fm: Formation; Volc: volcanic; unk: unknown; na: not applicable (partly from Muchez et al., 2008; Haest et al., 2009b; El Desouky et al., 2010; Van Wilderode et al., 2013).

4. Methodology

4.1 Strontium isotopic analysis

Carbonate powders (100 mg) from barren rocks and gangue minerals of the Kambove mineralisation were digested on a hot plate in 6 M HCl. Sr was isolated using Eichrom Sr Spec resin according to the procedure of De Muynck et al. (2009). $^{87}Sr/^{86}Sr$ ratios were determined using a Thermo Scientific NEPTUNE multi-collector inductively coupled plasma mass spectrometer (MC-ICP-MS, UGent) and normalised to the invariant $^{86}Sr/^{88}Sr$ ratio of 0.1194. Repeated analyses of the NIST SRM 987 isotopic reference material during the measurements yielded an $^{87}Sr/^{86}Sr$ ratio of 0.71030 ± 0.00008 (2s, n=41), in agreement with the accepted $^{87}Sr/^{86}Sr$ ratio of 0.71025 ± 0.00001 (Thirlwall, 1991). Two procedural blanks showed insignificant intensities compared to standard and sample solutions (< 0.1 %). Errors on the $^{87}Rb/^{86}Sr$ ratio are below 2%. Rb and Sr concentrations were determined using a Perkin-Elmer SCIEX ELAN 5000 quadrupole-based ICP-MS instrument. Rb-Sr data for the Kamoto and Luiswishi deposits were reported by Muchez et al. (2008) and El Desouky et al. (2010), for the Dikulushi deposit by Haest et al. (2009b), and for Kipushi by Van Wilderode et al. (2013).

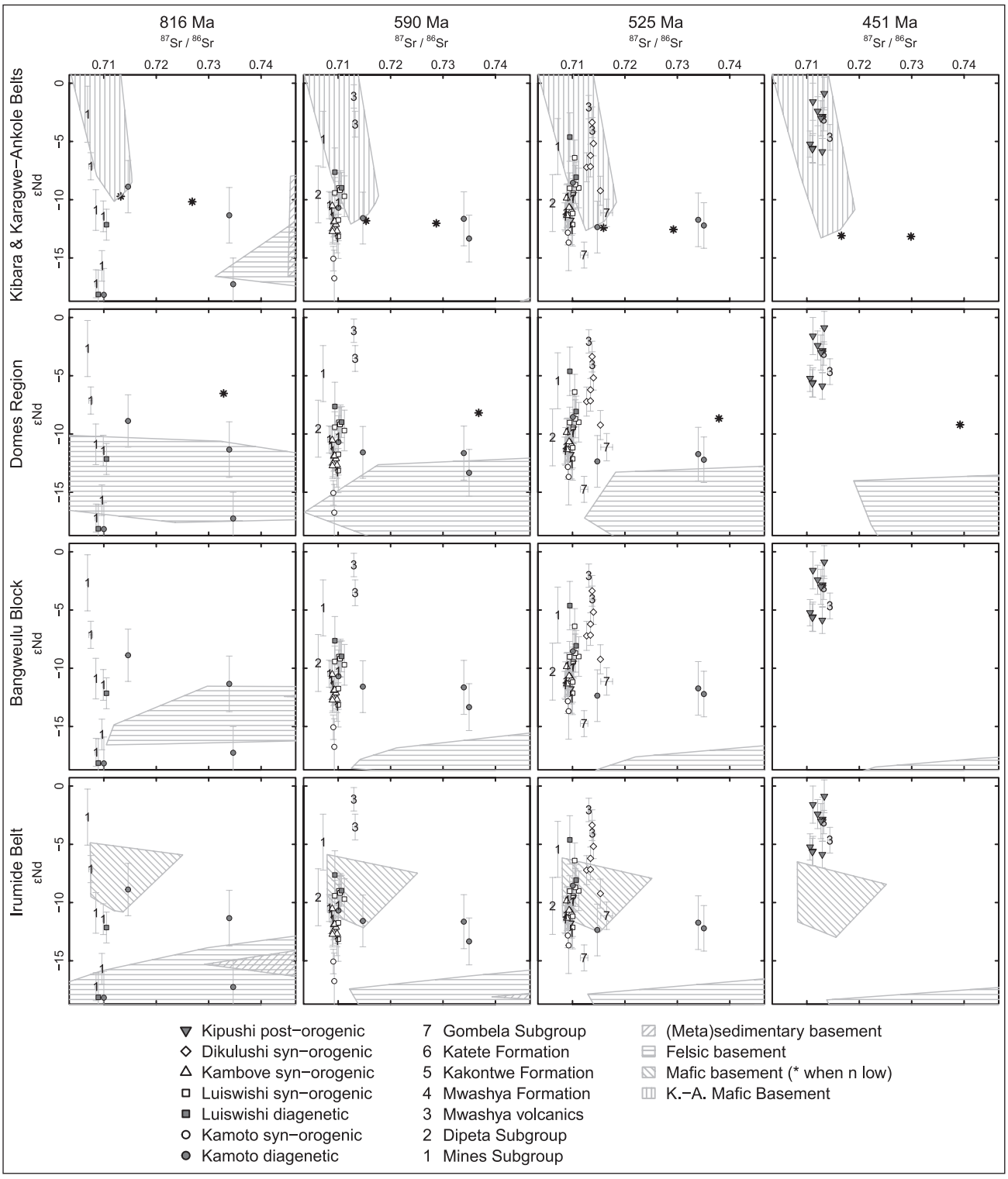

Figure 3. εNd vs $^{87}Sr/^{86}Sr$ diagrams at relevant ages with reference to different basement units. Basement data are grouped according to rock type. Data of Duchesne et al. (n=12; 2004) for the Karagwe-Ankole Belt (K.-A.; formerly North-Eastern Kibara Belt) are shown in the same diagrams as data for the Kibara Belt (n=23) and data from De Waele et al. (n=19; 2006) are combined with own results for the Irumide Belt (n=10) and Bangweulu Block (n=14). For the Domes Region, n=19. 2s-errorbars, obtained via error propagation, are not drawn when smaller than sample symbols.

4.2 Neodymium isotopic analysis

About 100 mg of carbonate powder was dissolved in 6 M HCl on a hotplate at 120°C. The evaporated residue was taken up into 2 M HNO_3. Nd was isolated using two columns containing Eichrom TRU Spec and Ln Spec resins according to procedures developed by Pin et al. (1994) and Ganio et al. (2012). The Nd isotopic composition was determined using a Thermo Scientific NEPTUNE MC-ICP-MS instrument (UGent) operated in static multi-collection mode. All Nd isotope ratios were normalised to $^{146}Nd/^{144}Nd = 0.7219$. Repeated measurements of JNdi-1 reference material (Geological Survey of Japan) yielded a $^{143}Nd/^{144}Nd$ ratio of 0.51211 ± 0.00001 (2s, n = 40), in agreement with the accepted ratio of 0.512115 ± 0.000007 (Tanaka et al., 2000). Two procedural blanks revealed insignificant intensities compared to standard and sample solutions (< 0.1 %). Errors on the $^{147}Sm/^{144}Nd$ ratio are below 4%. The Sm and Nd elemental concentration was measured with a Thermo Scientific ELEMENT XR single-collector sector field ICP mass spectrometer.

5. Results

5.1 Strontium isotopic analysis

Regarding the stratiform Cu-Co deposits of Kamoto and Luiswishi, the gangue carbonates of the diagenetic mineralisation phase show $^{87}Sr/^{86}Sr$ ratios at 816 Ma between 0.70894 ± 0.00012 and 0.73467 ± 0.00004 (n=17; Table 2; Fig. 3, 4). The isotope ratios of all diagenetic gangue carbonates are more radiogenic than the Sr isotopic composition of Neoproterozoic marine carbonates ($0.7056 < ^{87}Sr/^{86}Sr < 0.7087$; Jacobsen & Kaufman, 1999). The gangue minerals of the syn-orogenic mineralisation phase at Kamoto, Luiswishi and Kambove West have signatures at 525 Ma between 0.70875 ± 0.00002 and 0.71119 ± 0.00001 (n=22). For the vein-type mineralisation at Dikulushi, the $^{87}Sr/^{86}Sr$ ratios of syn-orogenic gangue dolomite at 525 Ma lie between 0.71270 ± 0.00001 and 0.71533 ± 0.00002 (n=7). Post-orogenic gangue dolomites from Kipushi have $^{87}Sr/^{86}Sr$ ratios at 451 Ma between 0.71061 ± 0.00002 and 0.71332 ± 0.00001 (n=9). Rb concentrations and $^{87}Rb/^{86}Sr$ ratios were measured for samples with radiogenic $^{87}Sr/^{86}Sr$ signatures or low Sr concentrations (Table 2). They show little influence of in situ ^{87}Rb decay, resulting in small age corrections. Furthermore, barren rock samples belonging to the Mines Subgroup (n=7), Dipeta Subgroup (n=5), Mwashya Subgroup (n=4), Kakontwe Formation (Muombe Subgroup; n=19), Katete Formation (Bunkeya Subgroup; n=1), and Gombela Subgroup (n=4) have been analysed (Table 2).

5.2 Neodymium isotopic analysis

For the stratiform Cu-Co deposits, $^{143}Nd/^{144}Nd$ ratios of diagenetic dolomites lie between 0.51066 and 0.51113 at 816 Ma, corresponding to εNd values between -18.2 ± 2.3 and -8.9 ± 2.2 (n=6; Table 3; Fig. 3). Syn-orogenic dolomites show $^{143}Nd/^{144}Nd$ signatures ranging from 0.51126 to 0.51163 at 525 Ma (n=16), or εNd values from -13.7 ± 2.4 to -6.4 ± 1.5. Syn-orogenic $^{143}Nd/^{144}Nd$ ratios for gangue minerals of the vein-type mineralisation at Dikulushi are between 0.51149 and 0.51179 at 525 Ma (n=6), equivalent to εNd between -9.2 ± 1.2 and -3.4 ± 1.3. Post-orogenic gangue minerals at Kipushi have $^{143}Nd/^{144}Nd$ ratios between 0.51176 and 0.51201 at 451 Ma (n=9), or εNd between -5.9 ± 1.1 and -0.9 ± 1.4. Table 3 also shows results for barren rocks of the Mines Subgroup (n=6), Dipeta Subgroup (n=1), Mwashya Subgroup (n=3) and Gombela Subgroup (n=4).

6. Discussion

6.1 Diagenetic mineralisation phase

Fig. 3 presents the isotope ratio data in εNd vs $^{87}Sr/^{86}Sr$ diagrams, with the gangue carbonates plotted at relevant ages and in comparison with the host rocks and different basement units. The basement dataset (unpublished) is divided into fields of felsic igneous, mafic igneous and (meta)-sedimentary rocks. The diagenetic gangue minerals are plotted at 816 Ma (Fig. 3). 816 ± 62 Ma is a six-point Re–Os isochron age obtained from chalcopyrite of the Konkola deposit (Barra & Broughton, in Selley et al., 2005). This is the oldest published age for the Cu–Co ore deposits in the Copperbelt and in agreement with a diagenetic origin (Selley et al., 2005). In addition, unpublished detrital zircon studies suggest formation of the host rocks between 840 and 790 Ma (Selley, in Hitzman et al., 2010). The diagenetic gangue carbonates of the Kamoto and Luiswishi deposits have varying isotopic compositions (Fig. 3, at 816 Ma). The distinctly high radiogenic Sr values ($^{87}Sr/^{86}Sr > 0.73$) of two Kamoto samples are reliable, since they contain comparably low Rb concentrations like the less radiogenic samples (i.e. less than 1 ppm; Table 2). The gangue carbonates cannot simply be correlated with a single basement unit, although the Domes Region might represent a best average composition. They do show a typical felsic signature regarding their generally low εNd values. This supports the interpretation of Muchez et al. (2008) that the mineralising fluids interacted significantly with felsic basement rocks or sedimentary rocks derived from it. According to Haest & Muchez (2011), the compositional variation of such rocks and incomplete mixing of the fluids might have caused the variable Pb isotopic signatures measured in ore sulphides. Similar processes might be invoked for the variable Nd and Sr isotopic composition of the gangue carbonates. Such interaction with felsic rocks can account for the leaching and enrichment of Cu, however, it is not expected to give rise to the high Co content of the deposits. Co is most likely derived from mafic rocks (e.g. Annels & Simmonds, 1984). The isotopic signature might have been partly overprinted, although a single εNd value of -8.9 ± 2.2 for a sample from Kamoto may point to a metal contribution of mafic basement material.

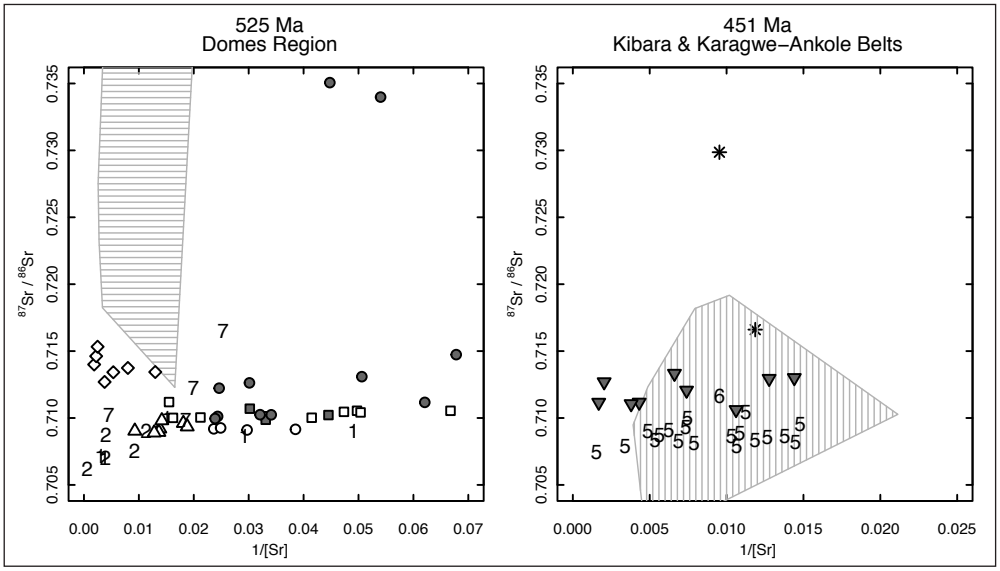

Figure 4. $^{87}Sr/^{86}Sr$ vs 1/Sr at 525 and 451 Ma, with reference to rocks of three basement units. Both figures are cropped to ranges containing most data points (legend as in Fig. 3).

Location	Timing/ ID	Mineralisation	Gangue type/ stratigraphy	Sm (µg/g)	2s	Nd (µg/g)	2s	$^{143}Nd/^{144}Nd$	2s	$^{147}Sm/^{144}Nd$	εNd 816 Ma	2s	εNd 590 Ma	2s	εNd 525 Ma	2s	εNd 451 Ma	2s	εNd 100 Ma	2s
	Post-orogenic																			
Dikulushi	DI04MH32	Cu-Ag	Cal 3	3,5	0,2	9,7	0,8	0,51187	0,00007	0,2159	na	na	na	na	na	na	na	na	-15,3	1,3
Dikulushi	DI04MH42	Cu-Ag	Cal 3	5,33	0,02	22,32	0,08	0,51226	0,00006	0,1456	na	na	na	na	na	na	na	na	-6,6	1,2
Kipushi	KI04HC01[2]	Cu-Zn	Dol vein	3,58	0,07	7,67	0,07	0,51274	0,00010	0,2813	na	na	na	na	na	na	-2,8	1,9	na	na
Kipushi	KI04HC02	Cu-Zn	Dol vein	6,34	0,08	13,31	0,09	0,51278	0,00006	0,2871	na	na	na	na	na	na	-2,4	1,2	na	na
Kipushi	KI04HC07	Cu-Zn	Dol vein	1,377	0,005	5,01	0,02	0,51225	0,00006	0,1677	na	na	na	na	na	na	-5,9	1,1	na	na
Kipushi	KI04HC10	Cu-Zn	Dol vein	0,705	0,002	2,56	0,01	0,51229	0,00006	0,1678	na	na	na	na	na	na	-5,2	1,1	na	na
Kipushi	KI04HC15	Cu-Zn	Dol vein	0,954	0,003	2,96	0,01	0,51236	0,00006	0,1978	na	na	na	na	na	na	-5,6	1,3	na	na
Kipushi	KI04HC16	Cu-Zn	Dol vein	0,940	0,003	3,08	0,01	0,51231	0,00006	0,1843	na	na	na	na	na	na	-5,7	1,2	na	na
Kipushi	KI04HC20	Cu-Zn	Dol vein	5,41	0,07	10,48	0,07	0,51293	0,00007	0,3114	na	na	na	na	na	na	-0,9	1,4	na	na
Kipushi	KI04HC28	Cu-Zn	Dol vein	3,87	0,05	7,47	0,05	0,51283	0,00008	0,3127	na	na	na	na	na	na	-3,0	1,5	na	na
Kipushi	KI04HC59	Cu-Zn	Dol vein	5,01	0,07	11,38	0,08	0,51276	0,00008	0,2663	na	na	na	na	na	na	-1,6	1,6	na	na
	Syn-orogenic																			
Dikulushi	DI04MH11	Cu-Pb-Zn-Fe	Cal 1	14	1	54	4	0,51226	0,00005	0,1638	na	na	na	na	-5,2	1,1	na	na	-7,0	1,1
Dikulushi	DI04MH17	Cu-Pb-Zn-Fe	Cal 1	52	4	177	14	0,51220	0,00006	0,1768	na	na	na	na	-7,2	1,2	na	na	-8,3	1,2
Dikulushi	DI04MH40	Cu-Pb-Zn-Fe	Dol 3	22	2	47	4	0,51264	0,00005	0,2893	na	na	na	na	-6,2	1,0	na	na	-1,2	1,0
Dikulushi	DI06MH34	Cu-Pb-Zn-Fe	Dol 3	4,2	0,3	18,4	1	0,51227	0,00007	0,1407	na	na	na	na	-3,4	1,3	na	na	-6,4	1,3
Dikulushi	DI06MH89	Cu-Pb-Zn-Fe	Dol 3	2,5	0,2	4,0	0,3	0,51279	0,00006	0,3781	na	na	na	na	-9,2	1,2	na	na	0,6	1,2
Dikulushi	DI06MH143	Cu-Pb-Zn-Fe	Cal 1	5,4	0,4	17,8	1	0,51222	0,00005	0,1829	na	na	na	na	-7,2	0,9	na	na	-7,9	0,9
Kambove	KW11SL01	Cu-Co	Dol III	1,8	0,2	3,15	0,06	0,51263	0,00006	0,3590	na	na	-12,5	1,2	-11,2	1,1	na	na	na	na
Kambove	KW11SL02	Cu-Co	Dol III	1,3	0,2	2,29	0,04	0,51265	0,00007	0,3599	na	na	-12,1	1,4	-10,8	1,4	na	na	na	na
Kambove	KW11SL03	Cu-Co	Dol III	0,9	0,1	1,86	0,04	0,51248	0,00006	0,3141	na	na	-11,9	1,3	-10,9	1,3	na	na	na	na
Kambove	KW11SL05	Cu-Co	Dol III	1,9	0,2	2,92	0,06	0,51280	0,00005	0,4059	na	na	-12,7	1,1	-10,9	1,1	na	na	na	na
Kambove	KW11SL09	Cu-Co	Dol III	1,5	0,2	2,60	0,05	0,51263	0,00005	0,3630	na	na	-12,7	1,1	-11,3	1,1	na	na	na	na
Kambove	KW11SL25	Cu-Co	Dol III	2,2	0,3	4,07	0,08	0,51259	0,00006	0,3403	na	na	-11,9	1,2	-10,7	1,2	na	na	na	na
Kambove	KW11SL43	Cu-Co	Dol III	0,9	0,1	2,10	0,04	0,51241	0,00006	0,2767	na	na	-10,5	1,2	-9,9	1,2	na	na	na	na
Luiswishi	LS06HA009	Cu-Co	Dol vein	2,7	0,6	6	1	0,51247	0,00008	0,2816	na	na	-9,7	1,7	-9,0	1,7	na	na	na	na
Luiswishi	LS06HA016	Cu-Co	Dol vein	5,61	0,02	24,06	0,09	0,51197	0,00006	0,1427	na	na	-9,0	1,3	-9,4	1,3	na	na	na	na
Luiswishi	LS06HA023	Cu-Co	Dol vein	0,294	0,001	0,714	0,003	0,51238	0,00008	0,2498	na	na	-9,1	1,6	-8,7	1,6	na	na	na	na
Luiswishi	LS06HA043	Cu-Co	Nod II	0,817	0,003	2,027	0,008	0,51234	0,00007	0,2440	na	na	-9,4	1,3	-9,0	1,3	na	na	na	na
Luiswishi	LS06HA060	Cu-Co	Breccia	0,8	0,2	1,8	0,4	0,51230	0,00008	0,2645	na	na	-11,7	1,8	-11,2	1,7	na	na	na	na
Luiswishi	LS06HA070	Cu-Co	Dol vein	1,245	0,004	1,437	0,005	0,51346	0,00008	0,5308	na	na	-9,2	1,5	-6,4	1,5	na	na	na	na
Luiswishi	LS06HA108	Cu-Co	Dol vein	2,2	0,5	4,2	0,8	0,51243	0,00008	0,3176	na	na	-13,1	1,9	-12,1	1,8	na	na	na	na
Kamoto	KA05VD067	Cu-Co	Dol vein	2,302	0,008	3,02	0,01	0,51290	0,00005	0,4646	na	na	-15,1	1,1	-12,8	1,1	na	na	na	na
Kamoto	KA07HA05[2]	Cu-Co	Dol vein	0,905	0,003	0,970	0,004	0,51320	0,00012	0,5645	na	na	-16,7	2,4	-13,7	2,4	na	na	na	na
	Diagenetic																			
Luiswishi	LS06HA005	Cu-Co	Nod/layers I	3,82	0,01	7,60	0,03	0,51260	0,00007	0,3056	-12,1	1,3	-9,0	1,3	-8,1	1,3	na	na	na	na
Luiswishi	LS06HA067[2]	Cu-Co	Nod/layers I	0,515	0,002	0,555	0,002	0,51365	0,00011	0,5584	-18,1	2,1	-7,6	2,1	-4,6	2,1	na	na	na	na
Kamoto	KA07HA04[2]	Cu-Co	Nod/layers I	0,299	0,001	0,407	0,002	0,51309	0,00012	0,4541	-18,2	2,3	-10,7	2,3	-8,5	2,3	na	na	na	na
Kamoto	KA07HA20[2]	Cu-Co	Nod/layers I	6	1	20	4	0,51200	0,00011	0,1861	-11,3	2,4	-11,6	2,3	-11,7	2,3	na	na	na	na
Kamoto	KA07HA21[2]	Cu-Co	Nod/layers I	1,8	0,4	3,2	0,6	0,51248	0,00009	0,3314	-17,3	2,2	-13,3	2,0	-12,2	2,0	na	na	na	na
Kamoto	KA07HA22[2]	Cu-Co	Nod/layers I	8	2	46	9	0,51169	0,00011	0,1035	-8,9	2,2	-11,6	2,2	-12,4	2,2	na	na	na	na
	Host rocks																			
Dikulushi	DI06MH83	na	Gombela Sbgr	17	1	99	8	0,51157	0,00006	0,1056	na	na	na	na	-14,8	1,1	-15,6	1,1	-19,7	1,1
Dikulushi	DI06MH107	na	Gombela Sbgr	3,02	0,01	14,89	0,06	0,51182	0,00006	0,1241	na	na	na	na	-11,1	1,2	-11,8	1,2	-15,1	1,2
Dikulushi	DI06MH108	na	Gombela Sbgr	2,8	0,2	11,5	0,9	0,51186	0,00006	0,1489	na	na	na	na	-11,9	1,1	-12,4	1,1	-14,5	1,1
S-Katanga	RG157635	na	Gombela Sbgr	0,74	0,08	4,30	0,08	0,51184	0,00006	0,1095	na	na	na	na	-9,7	1,1	-10,6	1,1	-14,5	1,1
Shituru	RG157670	na	Mwashya volc	22	2	156	3	0,51216	0,00005	0,0868	na	na	-1,1	1,0	-2,0	1,0	-3,1	1,0	na	na
Shituru	RG157672	na	Mwashya volc	6,5	0,7	29,7	0,6	0,51221	0,00006	0,1332	na	na	-3,5	1,1	-4,0	1,1	-4,6	1,1	na	na
S-Katanga	RG157668	na	Mwashya Sbgr	0,14	0,02	0,79	0,02	0,51212	0,00008	0,1082	na	na	-3,5	1,6	-4,2	1,6	na	na	na	na
S-Katanga	RG157674[2]	na	Dipeta Sbgr	0,051	0,006	0,283	0,005	0,51180	0,00013	0,1072	na	na	-9,5	2,4	-10,3	2,4	na	na	na	na

Table 3. Sm-Nd results with recalculation of the isotopic compositions at 816, 590, 525 and 451 Ma (abbreviations as in Table 2; [2]: isotope ratios with low precision due to small sample volumes are taken as indicative).

Alternatively, anomalous high Co concentrations have been reported in some felsic basement rocks, e.g. 1000 ppm in Lufubu Schists in the Nchanga region (Mackenzie-Brown, in Sweeney et al., 1991). Host rocks of the Mines Subgroup have low radiogenic Sr isotopic compositions ($^{87}Sr/^{86}Sr < 0.70990$), but very variable εNd values. It is difficult to compare host and gangue carbonates from the same stratigraphic member, largely because a lack of corresponding samples. However, both host and gangue rocks display a large range in εNd, e.g. 8.6 ε-units for three samples from the grey R.A.T. and 8.4 ε-units for three gangue carbonates occurring in the S.D.B. member.

6.2 Syn-orogenic mineralisation phase

The age and duration of the Lufilian orogeny, as well as the structural style of deformation are highly debated. The data are therefore plotted at the onset of the orogeny during eclogite facies metamorphism at ~590 Ma (U-Pb age; Rainaud et al., 2005), and late in the orogenic evolution around 525 Ma, when deformation could have reached Dikulushi in the foreland (Haest et al., 2009b; Fig. 3). During this period, the isotopic signature of syn-orogenic gangue minerals from Kambove West, both diagenetic and syn-orogenic gangue carbonates from Luiswishi, and the host rocks of the Mines Subgroup cluster together. The diagenetic carbonates from Kamoto also plot in that cluster, except for two samples with very radiogenic Sr isotopic signatures. The fact that both samples have εNd values similar to the cluster and that comparable low Sr concentrations are observed in an $^{87}Sr/^{86}Sr$ versus 1/Sr diagram (Fig. 4), probably indicates that they were influenced by a (local) fluid characterised by a radiogenic Sr signature. The clustering of the isotopic signatures points to remobilisation of diagenetic ore sulphides and strong interaction of the mineralising fluid with the host rocks during syn-orogenic mineralisation. Pitcairn et al. (2006) demonstrated the capacity of metamorphic fluids to mobilise metals. The importance of ore and/or iron sulphide remobilisation is supported by sulphur isotope ratios for Kamoto and Luiswishi, which partly formed by bacterial sulphate reduction (El Desouky et al., 2009). This is impossible at the high temperatures of the syn-orogenic mineralisation phase and must be the result of remobilisation. In addition, the diagenetic and syn-orogenic ore mineralogy is very similar (El Desouky et al., 2009). However, the syn-orogenic gangue carbonates from Kamoto have lower εNd values than the clustering samples. Although it concerns only two samples, this might be an indication that the mineralising fluid interacted with felsic basement, presumably the same as for the diagenetic mineralisation. Whether this resulted in a renewed contribution of metals is uncertain. Kamoto lies at the far west side of the Copperbelt, where the metamorphic grade did not reach the levels attained in the south-eastern Copperbelt. The rare earth element characteristics of carbonate gangue minerals reflect this metamorphic gradient (Debruyne et al., 2013) and dolomite recrystallisation was less significant at Kamoto than at Luiswishi (El Desouky et al., 2009). Regarding such reworking features, the Kambove West deposit resembles the Luiswishi deposit more closely. Hence, if the syn-orogenic mineralisation system was not restricted to the Katanga sedimentary cover, but also involved the basement, it is not a surprise that the evidence of this remains present in western deposits like Kamoto. The good agreement of isotopic signatures from western (Kamoto), central (Kambove) and eastern (Luiswishi) deposits in any case suggests a strong remobilisation event throughout the Katanga Copperbelt. No specific basement unit can be correlated to the clustering samples, only the isotopic composition of mafic rocks from the Irumide or Karagwe-Ankole Belts match partly. Considering the rather large distances of these belts (especially the latter) to the deposits and the convincing evidence for remobilisation, they are not thought to be involved. Mafic Mwashya volcanic rocks have clearly different isotopic compositions and are not part of the mineralising system (Fig. 3).

Syn-orogenic vein-type Cu-Pb-Zn-Fe mineralisation occurred at Dikulushi around 525 Ma. The gangue minerals have a homogeneous Sr isotopic composition ($0.71270 \pm 0.00001 < {}^{87}Sr/{}^{86}Sr < 0.71533 \pm 0.00002$), while the εNd values vary between -9.2 ± 1.2 and -3.4 ± 1.3. Four samples from the Gombela Subgroup host rocks plot at the lower end of this Nd isotopic trend, whereas the higher end has a typical mafic composition like the basic rocks from the Karagwe-Ankole Belt. In addition, two samples from mafic Mwashya volcanic rocks plot at the extension of the trend. The isotopic signatures of the gangue carbonates therefore possibly lie on a mixing line resulting from interaction of the mineralising fluid with the local host rocks and mafic rocks from the Mwashya volcanic series or similar mafic suites. Within the Dikulushi mine, Haest et al. (2007) described basalt fragments in a breccia at a fault zone. These local basaltic and siliciclastic host rocks are a viable influence on the isotopic signature of the mineralising fluid, rather than a distant basement. Whether they were also able to provide the ore metal budget for the mineralisation is uncertain. However, Haest et al. (2010) inferred from Pb isotope ratio data that the Pb content of this mineralisation phase was mobilised from local and isotopically inhomogeneous clastic reservoirs.

6.3 Post-orogenic mineralisation phase

The gangue carbonates of the Kipushi Cu-Zn deposit have radiogenic $^{87}Sr/^{86}Sr$ ratios, which may be derived from local phyllosilicate-rich stratigraphic layers (Van Wilderode et al., 2013). They plot at high εNd values, resulting in isotopic signatures corresponding to the mafic Mwashya volcanics and to mafic rocks from the Karagwe-Ankole Belt (Fig. 3). The Sr concentration of the former is much lower than found in the gangue carbonates (outside the range of Fig. 4), however, this could also be due to post-depositional processes. The Sr concentration of the latter was high enough to supply the Sr in the mineralising fluid (Fig. 4). Given the large distance of the Karagwe-Ankole Belt to Kipushi, its mafic rocks most likely did not contribute metals to the deposit, but they serve as a good indication that a similar mafic source rock may have provided the ore metals. The slabs of gabbro found in the axial breccia (De Magnée & François et al., 1988) might be the required mafic source. However, Heijlen et al. (2008) measured high Ba, Fe, Zn and Pb to Na ratios in fluid inclusions and suggested a felsic basement as source rock. The mineralising fluid therefore most likely interacted with both unidentified felsic basement rocks and mafic rocks occurring within the Axial Breccia (Van Wilderode et al., 2013). Whether the mafic rocks only altered the isotopic composition or also contributed metals to the fluid is uncertain.

Post-orogenic mineralisation at Dikulushi resulted in a Cu-Ag deposit. Pb isotope ratio systematics indicate that possibly around 100 Ma, both radiogenic Pb derived from local host rocks, and remobilised, less radiogenic Pb from the syn-orogenic ore went into the sulphides of the Cu-Ag deposit (Haest et al., 2010). Furthermore, the U-Th-Pb systems of the basalts occurring in the Dikulushi mine are disturbed at the same time, possibly meaning that they acted as additional sources of Cu and Ag (Haest et al., 2010). Two samples of gangue carbonates, predating but possibly associated with the Cu-Ag mineralisation (cal 3; Haest et al., 2009a), have very different εNd values at 100 Ma, i.e. -6.6 ± 1.2 and -15.3 ± 1.3 (not shown; Table 3). These signatures are similar to those of the syn-orogenic gangue minerals and the Gombela Subgroup host rocks at 100 Ma, respectively. This provides additional evidence for both remobilisation of precursor ore and interaction with the local host rock.

7. Conclusion

The basement beneath the Central African Copperbelt forms the most viable metal source for the numerous ore deposits in the region. Gangue carbonates of the diagenetic stratiform Cu-Co mineralisation phase show variable Sr and Nd isotopic compositions, but match best with felsic basement rocks, as exposed in the Domes Region. The origin of Co, which is typically derived from mafic rocks, remains uncertain. Homogeneous radiogenic isotope ratios, sulphur isotope ratios and the similar ore mineralogy indicate that the syn-orogenic mineralisation phase resulted from remobilisation of diagenetic sulphides. Few samples from the syn-orogenic phase at Kamoto have somewhat deviating isotopic signatures. This might point to additional, renewed input from felsic basement rocks. The higher metamorphic grade and resulting more pervasive remobilisation might mask this contribution in deposits lying in the central and eastern parts of the Katanga Copperbelt. The Sr and Nd isotopic composition of gangue minerals of the syn-orogenic, vein-type Cu-Pb-Zn-Fe mineralisation at Dikulushi lie on a mixing line between the isotopic signatures of the Gombela Subgroup host rocks and typical mafic rocks. The basalts occurring within the Dikulushi mine most likely represent the latter. Also Pb isotopic analyses indicated that these basalts acted as metal source (Haest et al., 2010). The mineralising fluid of the post-orogenic Cu-Zn deposit at Kipushi interacted with mafic rocks, most likely the gabbros occurring nearby. However, high Ba, Fe, Zn and Pb to Na ratios in fluid inclusions convincingly point towards a felsic metal source (Heijlen et al., 2008). Whether the gabbros contributed metals to the fluid or merely altered its isotopic signature is unclear.

8. Acknowledgements

The Royal Museum for Central Africa (RMCA, Tervuren) is thanked for permission to study the collections of P. Antun (Kipushi) and A. François and P. Antun (Katanga stratigraphy). Forrest International Group (G.F.I.) and Compagnie Minière du Sud Katanga (C.M.S.K.) allowed investigation of the Luiswishi samples and prof. dr. Eric Pirard (University of Liège, Belgium) provided samples of the Kamoto deposit. Sampling of the Kambove and Dikulushi deposits was permitted by the Société de Gécamines and Anvil Mining Congo, respectively. We are grateful to K. Latruwe for technical assistance during MC-ICP-MS measurements. This research is financially supported by Agency for Innovation by Science and Technology (IWT), research grant ZKC2784-00-W01, and Research Foundation - Flanders (FWO), research grants G.0414.08 and G.A078.11N.

9. References

Annels, A.E., 1974. Some aspects of the stratiform ore deposits of the Zambian Copperbelt and their genetic significance. In Bartholomé, P. (ed.), Gisements stratiformes et provinces cuprifères. Société Géologique de Belgique, Liège, 235-254.

Annels, A.E., 1989. Ore genesis in the Zambian Copperbelt with particular reference to the Northern Sector of the Chambishi Basin. In Boyle, R.W., Brown, A.C., Jefferson, C.W., Jowett, E.C. & Kirkham, R.V. (eds), Sediment-hosted Stratiform Copper Deposits. Geological Association of Canada, Special Paper, 36, 427-452.

Annels, A.E. & Simmonds, J.R., 1984. Cobalt in the Zambian Copperbelt. Precambrian Research, 25, 75-98.

Annels, A.E., Vaughan, D.J. & Craig, J.R., 1983. Conditions of ore mineral formation in certain Zambian Copperbelt deposits with special reference to the role of cobalt. Mineralium Deposita, 18, 71-88.

Andersen, L.S. & Unrug, R., 1984. Geodynamic evolution of the Bangweulu Block, northern Zambia. Precambrium Research, 25, 187-212.

Armstrong, R.A., Master, S. & Robb, L.J., 2005. Geochronology of the Nchanga Granite, and constraints on the maximum age of the Katanga Supergroup, Zambian Coperbelt. Journal of African Earth Sciences, 42, 32-40.

Bartholomé, P., Evrard, P., Katekesha, F., Lopez-Ruiz, J. & Ngongo, M., 1972. Diagenetic ore-forming processes at Kamoto, Katanga, Republic of the Congo. In Amstutz, G.C. & Bernard, A.J. (eds), Ores in Sediments, Springer-Verlag, Heidelberg, 21-41.

Bateman, A.M., 1930. Ores in the north Rhodesian Copperbelt. Economic Geology, 25, 365-418.

Batumike, M.J., Cailteux, J.L.H. & Kampunzu, A.B., 2007. Lithostratigraphy, basin development, base metal deposits, and regional correlations of the Neoproterozoic Nguba and Kundelungu rock successions, Central African Copperbelt. Gondwana Research, 11, 432-447.

Batumike, M.J., Kampunzu, A.B. & Cailteux, J.L.H., 2006. Petrology and geochemistry of the Neoproterozoic Nguba and Kundelungu Groups, Katangan Supergroup, southeast Congo: implication for provenance, paleoweathering and geotectonic setting. Journal of African Earth Sciences, 44, 97-115.

Bernau, R., Roberts, S., Richards, M., Nisbet, B., Boyce, A. & Nowecki, J., 2013. The geology and geochemistry of the Lumwana Cu (± Co ± U) deposits, NW Zambia. Mineralium Deposita, 48, 137–153.

Brown, A.C., 1984. Alternative sources of metals for stratiform copper deposits. Precambrium Research, 25, 61-74.

Cailteux, J.L.H., 1983. Le Roan Shabien dans le Région de Kambove (Shaba, Zaïre). Etude sédimentologique et métallogénique. Université de Liège, Belgique.

Cailteux, J.L.H., Kampunzu, A.B. & Lerouge, C., 2007. The Neoproterozoic Mwashya-Kansuki sedimentary rock succession in the central African Copperbelt, its Cu-Co mineralisation, and regional correlations. Gondwana Research, 11, 414-431.

Cailteux, J.L.H., Kaputo, A.K. & Kampunzu, A.B., 2003. Structure, lithostratigraphy and Cu-Co mineralization of the Mines Subgroup at Luiswishi, central Africa Copperbalt. In Cailteux, J.L.H. (ed.), Proterozoic sediment-hosted base metal deposits of Western Gondwana, Lubumbashi, 103-107.

Cailteux, J.L.H., Kampunzu, A.B., Lerouge, C., Kaputo, A.K. & Milesi, J.P. 2005. Genesis of sediment-hosted stratiform copper-cobalt deposits, central African Copperbelt. Journal of African Earth Sciences, 42, 134-158.

Cailteux, J., Binda, P.L., Katekesha, W.M., Kampunzu, A.B., Intiomale, M.M., Kapenda, D., Kaunda, C., Ngongo, K., Tshiauka, T. & Wendorff, M., 1994. Lithostratigraphical correlation of the Neoproterozoic Roan Supergroup from Shaba (Zaire) and Zambia, in the central African copper–cobalt metallogenic province. Journal of African Earth Sciences, 19, 265–278.

Carr, G.R., Dean, J.A., Korsch, M.J. & Mizon, K.J.,1987. A comparative study of the lead isotopic compositions of mineralization, basement rocks and gabbros from the Copperbelt and "Domes" regions of northern Zambia. Unpublished report, Commonwealth Scientific and Industrial Reasearch Organization, Division of Mineralogy and Geochemistry, Sydney, Australia.

Chabu, M., 1995. The geochemistry of phlogopite and chlorite from the Kipushi Zn-Pb-Cu deposit, Shaba, Zaire. Canadian Mineralogist, 33, 547-558.

Cosi, M., de Bonis, A., Gosso, G., Hunziker, J., Martinotti, G., Moratto, S., Robert, J.P. & Ruhlman, F., 1992. Late Proterozoic thrust tectonics, high-pressure metamorphism and uranium mineralization in the Domes area, Lufilian Arc, northwestern Zambia. Precambrian Research, 58, 215-240.

Debruyne, D., Balcaen, L., Vanhaecke, F. & Muchez, Ph., 2013. Rare earth element and yttrium characteristics of carbonates within the sediment-hosted Luiswishi and Kamoto Cu-Co deposits, Katanga Copperbelt (Democratic Republic of Congo - DRC). Geologica Belgica, 16, 76-83.

Dechow, E. & Jensen, M.L., 1965. Sulfur isotopes of some Central African sulfide deposits. Economic Geology, 60, 894-941.

Decrée, S., Deloule, E., De Putter, T., Dewaele, S., Mees, F., Yans, J. & Marignac, C., 2011. SIMS U-Pb dating of uranium mineralization in the Katanga Copperbelt: Constraints for the geodynamic context. Ore Geology Reviews, 40, 81-89.

Decrée, S., Deloule, E., Ruffet, G., Dewaele, S., Mees, F., Marignac, C., Yans, J. & De Putter, T., 2010. Geodynamic and climate controls in the formation of Mio-Pliocene world-class cobalt and manganese oxidized ores in the Katanga (DR Congo). Mineralium Deposita, 45, 621-629.

Dewaele, S., Muchez, Ph., Vets, J., Fernandez-Alonzo, M. & Tack, L., 2006. Multiphase origin of the Cu-Co ore deposits in the western part of the Lufilian fold-and-thrust belt, Katanga (Democratic Republic of Congo). Journal of African Earth Sciences, 46, 455-469.

Dewaele, S., Henjes-Kunst, F., Melcher, F., Sitnikova, M., Burgess, R., Gerdes, A., Fernandez-Alonso, M., De Clercq, F., Muchez, Ph., Lehmann, B., 2011. Late Neoproterozoic overprinting of the cassiterite and columbite-tantalite bearing pegmatites of the Gatumba area, Rwanda (Central Africa). Journal of African Earth Sciences, 61, 10-26.

De Magnée, I. & François, A., 1988. The origin of the Kipushi (Cu, Zn, Pb) deposits in direct relation with a Proterozoic salt diapir. Copperbelt of Central Africa, Shaba, Republic of Zaïre. In Friedrich, G.H. & Herzig, P.M. (eds), Base Metal Sulfide Deposits. Berlin Heidelberg, Springer-Verlag, 74-93.

De Muynck, D., Huelga-Suarez, G., Van Heghe, L., Degryse, P. & Vanhaecke, F., 2009. Systematic evaluation of a strontium-specific extraction chromatographic resin for obtaining a purified Sr fraction with quantitative recovery from complex and Ca-rich matrices. Journal of Analytical Atomic Spectrometry, 24, 1498-1510.

De Putter, T., Mees, F., Decrée, S. & Dewaele, S., 2010. Malachite, an indicator of major Pliocene Cu remobilization in a karstic environment (Katanga, Democratic Republic of Congo). Ore Geology Reviews, 38, 90-100.

De Waele, B. & Fitzsimons, I.C.W., 2007. The nature and timing of Palaeoproterozoic sedimentation at the southeastern margin of the Congo Craton; zircon U-Pb geochronology of plutonic, volcanic and clastic units in northern Zambia. Precambrian Research, 159, 95-116.

De Waele, B. & Mapani, B., 2002. Geology and correlation of the central Irumide belt. Journal of African Earth Sciences, 35, 385-397.

De Waele, B., Liégeois, J.P., Nemchin, A.A., Tembo, F., 2006. Isotopic and geochemical evidence of Proterozoic episodic crustal reworking within the Irumide Belt of south-central Africa, the southern metacratonic boundary of an Archaean Bangweulu Craton. Precambrian Research, 148, 225–256.

Duchesne, J.C., Liégeois, J.-P., Deblond, A. & Tack, L., 2004. Petrogenesis of the Kabanga-Musongati layered mafic-ultramafic intrusions in Burundi (Kibaran Belt): geochemical, Sr-Nd isotopic constraints and Cr-Ni behaviour. Journal of African Earth Sciences, 39, 133-145.

El Desouky, H.A., Muchez, Ph. & Cailteux, J., 2009. Two Cu-Co sulphide phases and contrasting fluid systems in the Katanga Copperbelt, Democratic Republic of Congo. Ore Geology Reviews, 36, 315-332.

El Desouky, H.A., Muchez, Ph., Boyce, A.J., Schneider, K., Cailteux, J.L.H., Dewaele, S. & von Quadt, A., 2010. Genesis of sediment-hosted stratiform copper-cobalt mineralization at Luiswishi and Kamoto, Katanga Copperbelt (Democratic Republic of Congo). Mineralium Deposita, 45, 735-763.

Fay, I. & Barton, M.D., 2012. Alteration and ore distribution in the Proterozoic Mines Series, Tenke-Fungurume Cu-Co district, Democratic Republic of Congo. Mineralium Deposita, 47, 501-519.

François, A., 1974. Stratigraphy, tectonique et minéralisations dans l'arc cuprifière du Shaba (République du Zaire). In Bartholomé, P. (ed.), Gisements stratiformes et provinces cuprifières. Liège, Belgium, Centenaire de la Société Géologique de Belgique, 79-101.

Ganio, M., Latruwe, K., Brems, D., Muchez, Ph., Vanhaecke, F. & Degryse, P., 2012. Sr-Nd isolation procedure for subsequent isotopic analysis using multi-collector ICP-mass spectrometry in the context of provenance studies on archaeological glass. Journal of Analytical Atomic Spectrometry, 27, 1335-1341.

Garlick, W.G., 1973. The Nchanga granite. In Lister, L.A. (ed.), Symposium on granites, gneisses and related rocks. Geological Society of South Africa, Special Publication, 3, 455–474.

Garlick, W.G., 1989. Genetic interpretation from ore relations to algal reefs in Zambia and Zaire. In Boyle, R.W., Brown, A.C., Jefferson, C.W., Jowett, E.C. & Kirkham, R.V. (eds), Sediment-hosted Stratiform Copper Deposits. Geological Association of Canada, Special Paper, 36, 471-498.

Garlick, W.C. & Brummer, J.J., 1951. The age of the granites of the northern Rhodesian Copperbelt. Economic Geology, 46, 478–498.

Gorjan, P., Veevers, J.J., Walter, M.R., 2000. Neoproterozoic sulfur-isotope variation in Australia and global implications. Precambrian Research, 100, 151-179.

Haest, M. & Muchez, Ph., 2011. Stratiform and vein-type deposits in the Pan-African orogen in central and southern Africa: Evidence for multiphase mineralisation. Geologica Belgica, 14, 23-44.

Haest, M., Muchez, Ph. & Dewaele, S., Francy, N. & Tyler, R., 2007. Metallogenesis of the Dikulushi Cu-Ag ore deposit in the Lufilian foreland (Democratic Republic of the Congo). Geologica Belgica, 10, 152-155.

Haest, M., Muchez, Ph., Petit, J.C.J. & Vanhaecke, F., 2009a. Cu isotope ratio variations in the Dikulushi Cu-Ag deposit, DRC: of primary origin or induced by supergene reworking? Economic Geology, 104, 1055-1064.

Haest, M., Muchez, Ph., Dewaele, S., Boyce, A.J., von Quadt, A. & Schneider, J., 2009b. Petrographic, fluid inclusion and isotopic study of the Dikulushi Cu-Ag deposit, Katanga (D.R.C.): implications for exploration. Mineralium Deposita, 44, 505–522.

Haest, M., Schneider, J., Cloquet, C., Latruwe, K., Vanhaecke, F. & Muchez, Ph., 2010. Pb isotopic constraints on the formation of the Dikulushi Cu-Pb-Zn-Ag mineralisation, Kundelungu Plateau (Democratic Republic of Congo). Mineralium Deposita, 45, 393-410.

Hanson, R.E., Wardlaw, M.S., Wilson, T.J. & Mwale, G., 1993. U-Pb zircon ages from the Hook granite massif and Mwembeshi dislocation: constraints on Pan-African deformation, plutonism, and transcurrent shearing in central Zambia. Precambrium Research, 63, 189-209.

Heijlen, W., Banks, D.A., Muchez, P., Stensgard, B.M. & Yardley, B.W.D., 2008. The nature of mineralizing fuids of the Kipushi Zn-Cu deposit, Katanga, Democratic Republic of Congo: quantitative fluid inclusion analysis using laser ablation ICP-MS and bulk crush-leach methods. Economic Geology 103, 1459-1482.

Hitzman, M.W., 2000. Source basins for sediment-hosted stratiform Cu deposits: implications for the structure of the Zambian Copperbelt. Journal of African Earth Sciences, 30, 855-863.

Hitzman, M.W., Selley, D. & Bull, S., 2010. Formation of sedimentary rock-hosted stratiform copper deposits through Earth history. Economic Geology, 105, 627-639.

Hitzman, M.W., Kirkham, R., Broughton, D., Thorson, J. & Selley, D., 2005. The sediment-hosted stratiform copper ore system. Economic Geology 100th Anniversary volume, 609−642.

Hurtgen, M.T., Arthur, M.A. & Halverson, G.P., 2005. Neoproterozoic sulfur isotopes, the evolution of microbial sulfur species, and the burial efficiency of sulfide as sedimentary pyrite. Geology, 33, 41-44.

Hurtgen, M.T., Arthur, M.A., Suits, N.S. & Kaufman, A.J., 2002. The sulfur isotopic composition of Neoproterozoic seawater sulfate: implications for a snowball Earth? Earth and Planetary Science Letters, 203, 413-429.

Jackson, M.P.A., Warin, O.N., Woad, W.M. & Hudec, M.R., 2003. Neoproterozoic allochthonous salt tectonics during the Lufilian orogeny in the Katangan Copperbelt, Central Africa. Geological Society of America Bulletin, 115, 314-330.

Jacobsen, S.B. & Kaufman, A.J., 1999. The Sr, C and O isotopic evolution of Neoproterozoic seawater. Chemical Geology, 161, 37-57.

John, T., Schenk, V., Mezger, K. & Tembo, F., 2004. Timing and PT evolution of whiteschist metamorphism in the Lufilian Arc-Zambezi belt orogen (Zambia): implications for the assembly of Gondwana. The Journal of Geology, 112, 71-90.

Kamona, A.F., Lévêque, J., Friedrich, G.H. & Haack, U., 1999. Lead isotopes of the carbonate-hosted Kabwe, Tsumeb and Kipushi Pb-Zn-Cu sulphide deposits in relation to Pan African orogenesis in the Damaran-Lufilian Fold Belt of Central Africa. Mineralium Deposita, 34, 273-283.

Kampunzu, A.B. & Cailteux, J., 1999. Tectonic evolution of the Lufilian Arc (Central Africa Copper Belt) during Neoproterozoic Pan African Orogenesis. Gondwana Research, 2, 401-421.

Kampunzu, A.B., Cailteux, J.H.L., Kamona, A.F., Intiomale, M.M. & Melcher, F., 2009. Sediment-hosted Zn-Pb-Cu deposits in the Central African Copperbelt. Ore Geology Review, 35, 263-297.

Kampunzu, A.B., Tembo, F., Matheis, G., Kapenda, D. & Huntsman-Mapila, P., 2000. Geochemistry and tectonic setting of mafic igneous units in the Neoproterozoic Katangan basin, central Africa: implications for Rodinia break up. Gondwana Research, 3, 125-153.

Kokonyangi, J.W., Kampunzu, A.B., Armstrong, R., Yoshida, M., Okudaira, T., Arima, M. & Ngulube, D.A., 2006. The Mesoproterozoic Kibaride belt (Katanga, SE D.R. Congo). Journal of African Earth Sciences, 46, 1-35.

Koziy, L., Bull, S., Large, R. & Selley, D., 2009. Salt as a fluid driver, and basement as a metal source, for stratiform sediment-hosted copper deposits. Geology, 37, 1107-1110.

Lefebvre, J.J., 1989. Les gisements stratiformes en roche sedimentaire d'Europe Centrale (Kupferschiefer) et de la ceinture cuprifère du Zaire et de Zambie. Annales de la Société Géologique de Belgique, 112, 121–135.

McGowan, R.R., Roberts, S., Foster, R.P., Boyce, A.J. & Coller, D., 2003. Origin of the copper-cobalt deposits of the Zambian Copperbelt: an epigenetic view from Nchanga. Geology, 31, 494-500.

Mendelsohn, F., 1961. Roan antilope. In Mendelsohn, F. (ed.), The geology of the Northern Rhodesian Copperbelt, MacDonald, London, 351-405.

Muchez, Ph. & Corbella, M., 2012. Factors controlling the precipitation of copper and cobalt minerals in sediment-hosted ore deposits: advances and restrictions. Journal of Geochemical Exploration, 118, 38-46.

Muchez, Ph., Vanderhaeghen, P., El Desouky, H., Schneider, K., Boyce, A., Dewaele, S. & Cailteux, J., 2008. Anhydrite pseudomorphs and the origin of stratiform Cu-Co ores in the Katangan Copperbelt (Democratic Republic of Congo). Mineralium Deposita, 43, 575-589.

Ngoyi, K. & Dejonghe, L., 1995. Geologie et genèse du gisement stratoide cuprifère de Kinsenda (SE du Shaba, Zaire). Bulletin de la Société belge de Géologie, 104, 245-281.

Ngoyi, K., Liégeois, J.-P., Demaiffe, D. & Dumont, P., 1991. Age tardi-ubendien (Protérozoïque inférieur) des dômes granitiques de l'arc cuprifère Zaïro-Zambien. Comptes Rendus des séances de l'Académie des Sciences, Paris, 313 (II), 83-89.

Omenetto, P., 1973. Mineralizzazioni cuprifere e granitizzazione: alcune osservazioni sui distretto di Mkushi (Zambia). Resoconti dell'Associazione Mineraria Sarda, 78,1–9.

Pienaar, P.J., 1961. Mineralization in the basement. In Mendelsohn, F. (ed.), The geology of the Northern Rhodesian Copperbelt. Macdonald, London, 30–41.

Pin, C., Briot, D., Bassin, C. & Poitrasson, F., 1994. Concomitant separation of strontium and samarium-neodymium for isotopic analysis in silicate samples, based on specific extraction chromatography. Analytica Chimica Acta, 298, 209-217.

Pitcairn, I.K., Craw, D., Olivo, G.R., Kerrich, R. & Brewer, T.S., 2006. Sources of metals and fluids in orogenic gold deposits: insights from the Otago and Alpine schists, New Zealand. Economic Geology, 101, 1525-1546.

Porada, H., 1989. Pan-African rifting and orogenesis in Southern to Equatorial Africa and Eastern Brazil. Precambrian Research, 44, 103–136.

Porada, H. & Berhorst, V., 2000. Towards a new understanding of the Neoproterozoic-Early Palaeozoic Lufilian and northern Zambezi Belts in Zambia and the Democratic Republic of Congo. Journal of African Earth Sciences, 30, 727-771.

Rainaud, C., Master, S., Armstrong, R.A., Phillips, D. & Robb, L.J., 2005. Monazite U-Pb dating and $^{40}Ar/^{39}Ar$ thermochronology of metamorphic events in the Central African Copperbelt during the Pan-African Lufilian Orogeny. Journal African Earth Sciences, 42, 183-199.

Richards, J.P., Cumming, G.L., Krstic, D., Wagner, P.A. & Spooner, E.T.C., 1988. Pb isotope constraints on the age of sulfide ore deposition and U-Pb age of late uraninite veining at the Musoshi stratiform copper deposit, Central African Copper Belt, Zaire. Economic Geology, 83, 724-741.

Roberts, S., Palmer, M.R., Cooper, M.J., Buchaus, P. & Sargent, D., 2009. REE and Sr isotope characteristics of carbonate within the Cu–Co mineralized sedimentary sequence of the Nchanga mine, Zambian Copperbelt. Mineralium Deposita, 44, 881–891.

Schneider, J., Melcher, F. & Brauns, 2007. Concordant ages for the giant Kipushi base metal deposit (DR Congo) from direct Rb-Sr and Re-Os dating of sulfides. Mineralium Deposita, 42, 791-797.

Schneiderhöhn, H., 1937. Die kupferlagerstätten von nord Rhodesia und Katanga. Geologische Rundschau, 28, 282–291.

Schuh, W., Leveille, R., Fay, I. & North, R., 2012. Geology of the Tenke-Fungurume sediment-hosted strata-bound copper-cobalt district, Katanga, Democratic Republic of Congo. Society of Economic Geologists, Special Publication 16, 269-301.

Selley, D., Broughton, D., Scott, R., Hitzman, M., Bull, S., Large, R., McGoldrick, P., Croaker, M., Pollington & N. & Barra, F., 2005. A new look at the Geology of the Zambian Copperbelt. Society of Economic Geologists, 100th anniversary Volume, 965-1000.

Sweeney, M.A. & Binda, P.L., 1989. The role of diagenesis in the formation of the Konkola Cu-Co orebody of the Zambian Copperbelt. Geological Association of Canada, Special Paper, 36, 499-518.

Sweeney, M.A. & Binda P.L., 1994. Some constraints on the formation of the Zambian Copperbelt deposits. Journal of African Earth Sciences, 19, 303-313.

Sweeney, M.A., Binda, P.L. & Vaughan, D.J., 1991. Genesis of the ores of the Zambian Copperbelt. Ore Geology Reviews, 6, 51-76.

Tack, L., Wingate, M.T.D., De Waele, B., Meert, J., Belousova, E., Griffin, B., Tahon, A. & Fernandez-Alonso, M., 2010. The 1375Ma "Kibaran event" in Central Africa: Prominent emplacement of bimodal magmatism under extensional regime. Precambrium Research, 180, 63-84.

Tanaka, T., Togashi, S., Kamioka, H., Amakawa, H., Kagami, H., Hamamoto, T., Yuhara, M., Orihashi, Y., Yoneda, S., Shimizu, H., Kunimaru, T., Takahashi, K., Yanagi, T., Nakano, T., Fujimaki, H., Shinjo, R., Asahara, Y., Tanimizu, M., Dragusanu, C., 2000. JNdi-1: a neodymium isotopic reference in consistency with LaJolla neodymium. Chemical Geology, 168, 279-281.

Thirlwall, M.F., 1991. Long-term reproducibility of multicollector Sr and Nd isotope ratio analysis. Chemical Geology 94, 85-104.

Unrug, R., 1988. Mineralization controls and source of metals in the Lufilian fold belt, Shaba (Zaire), Zambia, and Angola. Economic Geology, 83, 1247-1258.

Van Langendonck, S., Muchez, Ph., Dewaele, S., Kaputo Kalubi, A. & Cailteux, J., 2013. Petrographic and mineralogical study of the sediment-hosted Cu-Co ore deposit at Kambove West in the central part of the Katanga Copperbelt (DRC). Geologica Belgica, 16, 91-104.

Van Wilderode, J., Heijlen, W., De Muynck, D., Schneider, J., Vanhaecke, F. & Muchez, Ph., 2013. The Kipushi Cu-Zn deposit (DR Congo) and its host rocks: A petrographical, stable isotope (O, C) and radiogenic isotope (Sr, Nd) study. Journal of African Earth Sciences, 79, 143-156.

Veizer, J., Holser, W.T., Wilgus, C.K., 1980. Correlation of $^{13}C/^{12}C$ and $^{34}S/^{32}S$ secular variations. Geochimica et Cosmochimica Acta, 44, 579-587.

Wakefield, J.,1978. Samba: a deformed porphyry-type copper deposit in the basement of the Zambian Copperbelt. Transactions of the Institution of Mining and Metallurgy, 87, B43-B52.

Walshaw, R.D., Menuge, J.F. & Tyrell, S., 2006. Metal sources of the Navan carbonate-hosted base metal deposit, Ireland: Nd and Sr isotope evidence for deep hydrothermal convection. Mineralium Deposita, 41, 803-819.

Wendorff, M., 2000. Revision of the stratigraphical position of the "Roches Argilo-Talqueuses" (R.A.T.) in the Neoproterozoic Katangan Belt, south Congo. Journal of African Earth Sciences, 30, 717-726.

Wendorff, M., 2005. Evolution of Neoproterozoic–Lower Palaeozoic Lufilian Arc, Central Africa: a model based on syntectonic conglomerates. Journal of the Geological Society of London, 162, 5-8.

Whyte, R. & Green, M.,1971. Geology and paleogeography of Chibuluma West orebody. Economic Geology, 66, 411-424.

Manuscript received 06.11.2012, accepted in revised form 28.12.2013, available on line 01.02.2014